ON PICARD CRITERION AND THE WELL-POSED NATURE OF HARMONIC DOWNWARD CONTINUATION

JEFF CHAK FU WONG

February 2002

ON PICARD CRITERION AND THE WELL-POSED NATURE OF HARMONIC DOWNWARD CONTINUATION

Jeff Chak Fu Wong

Department of Geodesy and Geomatics Engineering
University of New Brunswick
P.O. Box 4400
Fredericton, N.B.
Canada
E3B 5A3

February 2002

PREFACE

This technical report is a reproduction of a thesis submitted in partial fulfillment of the requirements for the degree of Master of Science in Engineering in the Department of Geodesy and Geomatics Engineering, February 2002. The research was supervised by Dr. Petr Vanicek, and it was financially supported by the Natural Sciences and Engineering Research Council of Canada.

As with any copyrighted material, permission to reprint or quote extensively from this report must be received from the author. The citation to this work should appear as follows:

Dedication

To

my beloved parents -

Wong Tung Lung & Kan Siu Yin

Abstract

Harmonic downward continuation (HDC) is in the focus of this thesis. The main question we try to answer is whether the Helmert gravity anomaly reduction from the Earth's topography to the Helmert co-geoid through the Poisson surface integral is a well-posed problem or not. From the mathematical point of view, the Poisson surface integral is nothing else but a linear Fredholm integral equation of the first kind. Using the Helmert 2nd condensation technique, a transformation of the Stokes (geodetic) boundary value problem (GBVP) into the Helmert space is performed. Following that, the 3-D solution of the Helmert disturbing potential on and above the Helmert co-geoid is obtained by solving the (exterior) Dirichlet boundary value problem (DBVP) for the Laplace equation.

It is shown that the HDC, for the $5^{'} \times 5^{'}$ grid-size, is a well-posed problem in Hadamard's sense. Small variations of the Helmert gravity anomaly in the Earth's topography produce reasonably small variations of the Helmert gravity anomaly on the Helmert co-geoid when the first kind Fredholm integral equation is used.

In order to measure the "magnification" by the HDC, we provide an effective tool for analyzing the exact nature of this problem in the form of the Picard criterion. The Picard criterion is a technique that indicates whether the sequence of the ratio becomes convergent or divergent. In the core of this thesis, a technical question will be asked:

> "How do the properties of compact or discrete Picard criterion relate to the DBVP for the HDC problem? "

The answer to this question is important from both fundamental and practical points of view, because the criterion shows how the existence and stability estimate of the HDC problem can be used. The principles of the criterion are illustrated and the results of two applications are presented. For real-life application, we restrict ourselves to demonstrating a discrete case. Hence, we will be dealing with the discrete Picard

technique (DPT). We concentrate on the finite-dimensional non-symmetric matrix of the HDC arising from the discretization of the integral equation, which are related to an eigenvalue system, referred to as the quasi-eigenvalue decomposition (QEVD).

Numerical results are presented throughout the thesis to illustrate the applications of a DPT studied, with emphasis on stability and existence of the HDC problem.

Acknowledgments

I am deeply grateful to my supervisor, Prof. Dr. Petr Vaníček for introducing me to this beautiful subject of geodesy investigation, for his years of encouragement, his adept guidance, his infinite patience, without whose generous assistance this thesis could not have come into light. The opportunity to be one of his students is my great pleasure.

I am also indebted to Prof. Dr. Small and Prof. Dr. Santos, who spend their valuable time serving on my committee.

I owe many thanks to my parents and my other family members, Jackson, Jess and Ken for their many years of support in all possible means, especially, to my mother for her years of forever love, inspiration and patience who merely expects me to become an educated man.

I am so grateful to Mr. Jianliang Huang, and Mr. Pavel Novák for all the things I learned from them in the geoid meetings, seminars, private discussions. They always treated me as a baby-brother.

I am indebted to the (Lisa) McKnight, Lapoint and (Donna) Dykeman families who gave their valuable understanding and help.

Finally, my deepest gratitude goes to my friends all around the world. Mensur Omerbashich of Bosnia (and recently of the U.S.), Paul Collins of Britain, Jason Carter, Jonathan Carter, Helen Nancy Tanfara, Gwendy Dianne Harrington, Sunil Bisnath of Canada, Ashraf Mohamed Hemeida of Egypt, Edouard Kammérér, Sébastien Romet, David Rouison of France, Stefan Ulrich Malcus, Yves Albrecht,

Table of Contents

List of Tables

List of Figures

List of Symbols

In geodesy, the superscript of any physical quanlitlies denotes a specific type of given functional space while the subscript denotes the location of any physical quanlities.

List of commonly used nomenclatures

In the english alphabet

$\mathbf{B}$ - non-symmetrical coefficient matrix

$\mathbf{B}^{-1}$ - inversion of the non-symmetrical coefficient matrix

C_0 - spherical cap over the Earth

$D_{\Delta g^h}$ - truncation error of the truncated Poisson integration in spectral form

e - first eccentricity

$\mathbf{E}$ - East

f - geometrical flatterning of the reference ellipsoid

GM - geocentric gravitational constant

g^h - Helmert gravity

H^O - orthometric height

I - identity vector

I_{max} - cut-off degree of the modified Molodenskij-Poisson kernel

J_2 - second degree coefficient, representing the flattening of the reference (normal) ellipsoid

K - Poisson kernel

$\overline{K^m}$ - modified Molodenskij-Poisson kernel

$\overline{\overline{\mathbf{K}^m}}$ - doubly averaged (integrated) modified Poisson kernel

$\overline{Q_j}$ - modified Molodenskij-Poisson coefficients

$\hat{m}$ - geodetic parameter

N - North

$r_{c:g}$ - radial distance of the Helmert co-geoid from the center of the Earth

(r_t, Ω) - a point on the Earth's topography, r_t is the radial distance of the Earth's surface from the center of the Earth, $\Omega = (\varphi, \lambda)$ is the geocentric solid angle which is a function of geocentric co-latitude and longitude

$\mathbf{r}^{\mathrm{Num.}}_{\mathbf{B}_{\{I,II,III\}}}$ - difference between the given solution of **B** and computed solution of $\mathbf{B}\mathbf{V}\Lambda^+\mathbf{U}^T$

P_j - Legendre polynomials

R - mean radius of the Earth

t_j - modified Poisson kernel with unknown coefficients

T - disturbing potential

T^h - Helmert disturbing potential

$\mathbf{u}_i$ - left-eigenvectors of the matrix $\mathbf{B}$

U - reference normal gravity potential of the Somigliana-Pizzetti type

U^c - centriful acceleration potential

U^g - gravitational part of the normal potential

$\mathbf{u}_i^T$ - right-eigenvectors of the matrix $\mathbf{B}$

W - Earth gravity potential

W^c - centriful acceleration potential

W^g - gravitational (attraction) potential

W^h - Helmert gravity potential

W_0 - gauge value or constant value

Y_{jm} - spherical harmonic functions

Y_{jm}^* - complex conjugate of Y_{jm}

$Z^h(r_t, \Omega)$ - vertical displacement of the corresponding equipotential surfaces belonging to the two gravities

In the Greek alphabet

γ - normal gravity

Γ_e - region of the reference ellipsoid of revolution

Γ_t - Earth's topography

Δg - gravity anomaly

Δg^h - Helmert gravity anomaly

$\epsilon_{\delta g}$ - ellipsoidal correction for the gravity disturbance

ϵ_n - ellipsoidal correction for the normal gravity field

ϵ^{Num} - computed magnitude of the numerical errors

λ_i - eigenvalues of the matrix $\mathbf{B}$

ς_j - eigenvalues of $D_{g^h_{c:g}}$

ψ - spherical distance between two geocentric angles (Ω, Ω') on the surface of the unit sphere

ψ_0 - radius of spherical cap

Ω_i - different geocentric angles within the $3° \times 5°$ block

List of commonly used subscripts

$c : g$ - Helmert co-geoid

e - reference ellpsoid of revolution

i - dimensionality of the matrix

$\{I, II, III\}$ - three areas of coverage of the mean Helmert gravity data

j - degree

m - order

min - minimum

max - maximum

n - dimensionality of the matrix

t - Earth's topography

List of commonly used superscripts

L - high frequency part of Helmert gravity anomaly

T - transpose of an eigenvector

List of commonly used symbols

$\circ$ - degree

eps - computer machine precision

$\mathbb{H}$ - Helmert space

$\doteq$ - is approximated by

$\in$ - is belonging to

$\equiv$ - is equivalent to

$\neq$ - is not equal to

$\mathbb{R}^3$ - three-dimensional real space

$\mathbb{R}^{\cdot \times \cdot}$ - the set of $\cdot \times \cdot$ or $\cdot$ - by - $\cdot$ real matrics

$\mathbb{S}^2$ - two-dimensional Euclidean manifold of any well-suited sphere

List of Abbreviations

List of commonly used abbreviations

CPC - Compact Picard criterion

DBVP - Dirichlet boundary value problem

DPC - Discrete Picard criterion

DPT - Discrete Picard tecnhique

EVE - Eigenvalue expansion

FZC - Far zone contribution

GBV - Geodetic boundary value

GBVP - Geodetic boundary value problem

HDC - Harmonic downward continuation

QEVD - Quasi-eigenvalue decomposition

MPTK - Modified Molodenskij-Poisson truncation kernel

NZC - Near zone contribution

TE - Truncation error

Chapter 1

Definition of The Problem

1.1   Definition of The Problem To Be Solved

The classical formulation of the *geodetic boundary value problem* (GBVP) (Stokes, 1849; Heiskanen and Moritz, 1967; Sansò, 1977, 1997) for solving the disturbing potential[1] $T(r, \Omega)$ in harmonic space has been recently reformulated by Martinec *et al.* (1993, 1994a, 1994b, 1998) and Vaníček *et al.* (1994, 1996, 1999), and is known as the Stokes-Helmert scheme (Stokes, 1849; Helmert, 1884) for solving the GBVP. The beauty of the Stokes-Helmert formulation is the transformation of the GBVP into *Helmert space* IH, where the potential to be determined can be fulfilled by harmonicity of the Laplace equation using the Helmert 2nd condensation technique. This scheme is of special interest for the determination of the geoid imbedded in a

---

[1] The disturbing potential is generally expressed as (e.g., Vaníček and Krakiwsky, 1986):

$$T(r, \Omega) = W(r, \Omega) - U(r, \Omega),$$

where W is the Earth gravity potential, which is composed of gravitational (attraction) W^g and centrifugal acceleration W^c potentials, and U is the reference normal gravity potential of the Somigliana-Pizzetti type, which is composed of the gravitational part of the normal potential U^g and the centrifugal acceleration potential U^c. Whereas most people think of the centrifugal potential as being a harmonic function, they are wrong even though the potentials W^c and U^c will cancel each other out when one puts into Laplace's equation. The centrifugal potential is **not** a harmonic function (Moritz, 1992).

harmonic space, where the harmonic space is given as a *Helmert space* (Vaníček *et al.*, 1999).

A classical *geodetic boundary value*[2] (GBV), for example:

$$\frac{\partial T}{\partial h} + \frac{1}{\gamma}\frac{\partial \gamma}{\partial h}T = -\Delta g, \tag{1.1.1}$$

revisited earlier by Zagrebin (1956) was recently modified by Vaníček *et al.* (1999). The main modification is the transformation of the GBV into an equivalent form involving the Helmert gravity anomaly Δg^h and two ellipsoidal corrections ϵ_n and $\epsilon_{\delta g}$. In the Helmert space setting, the GBV is a problem, particularly for a first order non-homogeneous partial differential equation[3], which has values assigned on the physical boundary of the Earth's topography in which the problem is specified:

$$\frac{\partial T^h}{\partial r}\bigg|_{(r_t,\Omega)} + \frac{2}{r}T^h\bigg|_{(r_t,\Omega)} \doteq -\Delta g^h(r_t,\Omega) + \epsilon_n(r_t,\Omega) + \epsilon_{\delta g}(r_t,\Omega), \tag{1.1.2}$$

where $T^h(r_t,\Omega)$ denotes an unknown Helmert disturbing potential, (r_t,Ω) denotes a point on the Earth's topography, r_t is the radial distance of the Earth's surface from the center of the Earth, $\Omega = (\varphi, \lambda)$ is the geocentric solid angle which is a function of geocentric co-latitude and longitude. As put forward by Vaníček *et al.* (1999), the Helmert gravity anomaly on the Earth's topography is given as (the symbol := means that the left side is defined by the right one):

$$\Delta g^h(r_t,\Omega) := g^h(r_t,\Omega) - \gamma[(r_t - (Z^h(r_t,\Omega)),\Omega], \tag{1.1.3}$$

where $g^h(r_t,\Omega)$ denotes the Helmert gravity, and $\gamma[(r_t - (Z^h(r_t,\Omega)),\Omega]$ denotes the normal gravity located on the Helmert telluroid[4], and $[(r_t - (Z^h(r_t,\Omega)),\Omega]$ denotes the

---

[2]This is also referred to as the *Robin boundary value* (Dancer, 1998). The Robin boundary value is a third boundary value, which is a linear combination of the Dirichlet and Neumann boundary values (Gustafson and Abe, 1998a, 1998b).

[3]Physically speaking, the Helmert gravity anomaly with the two ellipsoidal corrections is composed of a part from the induced potential (or from the vertical gradient of Helmert gravity anomaly) and a part from the undeformed Helmert disturbing potential in multiplication with the inverse radial distance.

[4]The Helmert telluorid is defined as equipotential surface of the normal gravity field.

corresponding point (point in the same direction Ω) on the telluroid in the Helmert space, and $Z^h(r_t, \Omega)$ denotes the vertical displacement of the corresponding equipotential surfaces belonging to the two gravities. Throughout the thesis, we will adopt a geocentric coordinate reference system for describing the Helmert disturbing potentials (e.g., McCarthy, 1996).

As mentioned in the above paragraph, to have a proper procedure for constructing the GBV, two ellipsoidal corrections must be taken into account. First is the ellipsoidal correction for the gravity disturbance, $\epsilon_{\delta g}(r_t, \Omega)$, which comes from the difference between the derivative of the potential T^h with respect to the plumb line of the normal gravity field and the geocentric radial derivative of T^h, i.e.:

$$\epsilon_{\delta g}(r_t, \Omega) = -f \sin 2\varphi \left. \frac{1}{r} \frac{\partial T^h}{\partial \varphi} \right|_{(r_t, \Omega)}, \tag{1.1.4}$$

where f is the geometrical flattening of the reference ellipsoid, and φ is a geocentric co-latitude. Second is the ellipsoidal correction for the normal gravity field, $\epsilon_n(r_t, \Omega)$, which is derived from the second type of Bruns's formula (or the vertical gradient of the gravity) (e.g., Vaníček and Krakiwsky, 1986), i.e.:

$$\epsilon_n(r_t, \Omega) = -2 \left[\widehat{m} + f \left(\cos 2\varphi - \frac{1}{3} \right) \frac{T^h}{r} \right] \Bigg|_{(r_t, \Omega)}, \tag{1.1.5}$$

where $\widehat{m}$ is the geodetic parameter. Equations (1.1.4) and (1.1.5) have been extensively studied by Bruns (1878), Molodenskij (1949), Zakatov (1953), Zagrebin (1956), Jekeli (1981a), Cruz (1986), Heck (1991b), Vaníček and Martinec (1994), Martinec (1999), and Vaníček et al. (1999).

The left-hand side of Eq. (1.1.2) shows that a Helmert disturbing potential T^h is a harmonic function of a 3-D position. Equating Eq. (1.1.1) with Eq. (1.1.2) on the right-hand side gives:

$$\Delta g(r_t, \Omega) = \Delta g^h(r_t, \Omega) - \epsilon_n(r_t, \Omega) - \epsilon_{\delta g}(r_t, \Omega). \tag{1.1.6}$$

It is known that a product of the radial distance with Helmert's gravity anomalies

from the Earth's topography down to the Helmert co-geoid[5] is a harmonic function (mathematically speaking, $r_t \Delta g^h(r_t, \Omega)$ satisfies $\nabla^2 \left(r_t \Delta g^h(r_t, \Omega) \right) = 0$). Instead of taking the GBVP into account for determining the Helmert disturbing potential, we focus on the other boundary value problem introduced in geodetic literature for solving an unknown harmonic function that is used to take on prescribed values at points on the boundary, known as the *exterior Dirichlet (boundary value) problem* (DBVP) (e.g., Kellogg, 1926; 1967). Here, the problem is to find the Helmert gravity anomaly on the Helmert co-geoid $\Delta g_{c:g}^h(\Omega')$ (or $\Delta g_{c:g}^h(r_g, \Omega')$) continued downward from the first term in Eq. (1.1.7) when the linear Fredholm integral of the first kind has the form:

$$r_t \Delta g^h(r_t, \Omega) = \frac{r_{c:g}}{4\pi} \int_{\Omega'} \Delta g_{c:g}^h(\Omega') K(r_t, r_{c:g}; \Omega, \Omega') d\Omega', \qquad (1.1.7)$$

where $K(r_t, r_{c:g}; \Omega, \Omega')$ denotes the *Poisson kernel* and $r_{c:g}$ is the radial distance of the Helmert co-geoid from the center of the Earth. In other words, in order to compute $\Delta g_{c:g}^h(\Omega')$, surface gravity observations $\Delta g_t^h(\Omega)$ (or $\Delta g^h(r_t, \Omega)$) multiplied by the corresponding radial distances (or r_t), which are to be harmonic functions of 3-D position, must be downward continued through the Earth's topography to the Helmert co-geoid. This procedure is referred to as the *harmonic downward continuation* (HDC) problem. A question to be addressed is the uncertainty of whether or not a product of the radial distance with two ellipsoidal corrections is a harmonic function. The integral representation has the form:

$$r_t \left[\epsilon_n(r_t, \Omega) + \epsilon_{\delta g}(r_t, \Omega) \right] \overset{?}{=} \frac{r_{c:g}}{4\pi} \int_{\Omega'} \left[\epsilon_n(r_{c:g}, \Omega') + \epsilon_{\delta g}(r_{c:g}, \Omega') \right] K(r_t, r_{c:g}; \Omega, \Omega') d\Omega'.$$

$$(1.1.8)$$

---

[5]The geoid (Listing, 1873) is defined as an equipotential surface of the Earth's actual gravity field, inside topographical masses on land, more or less coinciding with the mean sea level at sea (Vaníček and Christou, 1994). In the actual space, there exists masses located above the geoid. Using the Helmert 2nd condensation technique, all the masses can be condensed in a layer. Hence, this transformation of the Earth's gravitational volume and surface potentials causes a shift of all equipotential surfaces. In the Helmert space setting, the shifted geoid is called a *Helmert co-geoid.*

We will not discuss here, but will extend in future to report the sum of two ellipsoidal corrections on the Earth's topography, which is a harmonic function of 3-D position.

The HDC problem has been studied in various formulations. We can find it described, for example, in Martinec (1996) or Vaníček *et al.* (1996) or more recently in Sun and Vaníček (1997, 1998). Through an extensive generalization of what Fredholm (1900) called a *linear* (now called Fredholm) *integral equation of the first kind*, the HDC offers a tool for determining the Helmert gravity anomaly on the Helmert co-geoid, which turns out to be a well-posed problem according to Hadamard (1902).

For a problem to be well-posed in the Hadamard sense, it must meet the following criteria:

1. For each given set of data, there exists a solution.

2. The solution is unique.

3. The solution depends continuously on the given data.

If a problem does not meet one (or more) of the above criteria the problem is considered to be ill-posed. The posedness of the HDC problems has been broadly investigated by many geodesists, e.g., Moritz (1966a, 1966b), Krarup (1969), Schwartz (1971, 1978), Grafarend (1972), Sjöberg (1975), Rummel and Gerstl (1979, 1981), Engl (1982), Neyman (1985), Ilk (1987, 1993), and Engles *et al.* (1993). A practical approach to the HDC problem where a discrete set of Helmert's gravity anomalies on the Earth's topography is continued downward on the Helmert co-geoid was put forward by Vaníček *et al.* (1996, 1999) and Martinec (1996). In the year of 1996, Martinec and Vaníček *et al.* independently confirmed that the HDC, for the $5^{'} \times 5^{'}$ point/mean Helmert gravity anomalies, is a well-posed problem.

When dealing with the HDC problem, one runs into a *stability estimate*, meaning that the Helmert gravity anomaly on the Helmert co-geoid (the output) depends continuously on the input. In other words, the output is stable under small modifications

of the Helmert gravity anomaly on the Earth's topography (the input). In order to measure the magnification by the HDC, one transfers the problem to be solved into a spectral form (or power series form or summation series form), known as the *Picard criterion* (1910). The Picard criterion is a technique that indicates whether the sequence of the ratio turns out to be convergent or divergent. These sequences can be extracted from a finite series expansion and a finite dimensional non-symmetric matrix. We restrict ourselves to demonstrating a discrete case. This restriction is imposed to facilitate the graphical description for analyzing the magnified difference between the input and the output. We will be referring to the Picard criterion as the *discrete Picard technique* (DPT). The DPT, modified by Hansen (1988, 1990), can also be used for demonstrating the existence of a solution to the HDC problem and associated with the numerical analysis.

For numerical demonstrations, as a spherical approximation, the radius of the Helmert co-geoid $r_{c:g}$ can be approximated by a sphere with the mean radius $R = 6371$ km of the Earth, i.e., $r_{c:g}(\Omega) = R$. The radius of the Earth's topography r_t is sum of R and an orthometric height $H^O(\Omega)$, i.e., $r_t(\Omega) = R + H^O(\Omega)$. This approximation is acceptable because the discrepancy generated from this approximation is at most 3×10^{-3} (Heiskanen and Moritz, 1967). Because of the above assumptions, a new expression of Eq. (1.1.7) can be written as:

$$r_t \Delta g^h(r_t, \Omega) = \frac{R}{4\pi} \int_{\Omega'} \Delta g_{c:g}^h(\Omega') K(r_t, R; \Omega, \Omega') d\Omega'. \qquad (1.1.9)$$

The goal of this thesis is to show how the discrete Picard technique can be used for analyzing the stability and existence of the HDC problem. First, the discrete Picard technique can be associated with the so-called eigenvalue system. Two eigenvalue systems are considered in order to determine two sets of eigenvalues, and eigenfunctions/eigenvectors. One is the *eigenvalue expansion* (EVE) (Schmidt, 1907; Smithies, 1937) of a *modified Molodenskij-Poisson truncation kernel* (MMPTK) $\overline{K}^m(H^O, \psi, \psi_0)$ in a spectral form (Molodenskij *et al.*, 1962; Vaníček *et al.*, 1991, 1996), where ψ is

a spherical (or an angular) distance between two geocentric angles on the surface of the unit sphere and ψ_0 is a radius of spherical cap. Thanks to the addition theorem, the MMPK[6] viz the EVE can written in terms of either the Legendre polynomials P_j or spherical harmonic functions Y_{jm} as:

$$
\overline{K}^m(H^O, \psi, \psi_0) = \sum_{j=2}^{I_{\max}} \frac{\overline{Q}_j(H^O, \psi_0)}{2} P_j(\cos\psi)
$$

$$
= \sum_{j=2}^{I_{\max}} \frac{\overline{Q}_j(H^O, \psi_0)}{2} \sum_{m=-j}^{j} Y_{jm}(\Omega) Y_{jm}^*(\Omega'), \qquad (1.1.10)
$$

where $\overline{Q}_j(H^O, \psi_0)$ is the modified Molodensij-Poisson coefficients (Vaníček *et al.*, 1996; Sun and Vaníček, 1998), $I_{\max}$ denotes as the cut-off degree of MMPK, $Y_{jm}^*(\Omega')$ denotes the complex conjugate of $Y_{jm}(\Omega')$. An eigenvalue system for $\overline{K}^m$:

$$
(Y_{jm}(\Omega), Y_{jm}^*(\Omega'); \overline{Q}_j(H^O, \psi_0)/2)_{\substack{2 \leq j \leq \infty, \\ -j \leq m \leq j}}, \qquad (1.1.11)
$$

is a sequence of spherical harmonic functions, $Y_{jm}(\Omega)$, $Y_{jm}^*(\Omega')$, called eigen-functions, and finite values of the coefficients $\overline{Q}_j(H^O, \psi_0)/2$, called eigenvalues, satisfying five properties (see Appendix A). The other is the *quasi-eigenvalue decomposition* (QEVD) of any arbitrary square matrix $\mathbf{B}$ (e.g., Bjerhammar, 1973; Golub and Van Loan, 1983; Ren, 1996), where $\mathbf{B}$ is a coefficient matrix which has a simple relation with the *doubly averaged (integrated) modified Poisson kernel* $\overline{\overline{\mathbf{K^m}}}$ multiplying with a scale factor (Vaníček *et al.*, 1996), i.e.:

$$
\mathbf{B} = \frac{R}{4\pi r_t} \overline{\overline{\mathbf{K^m}}}. \qquad (1.1.12)
$$

The non-symmetric matrix $\mathbf{B}$ viz the QEVD can be written in a spectral vector-form as:

$$
\mathbf{B} = \sum_{i=1}^{n} \lambda_i \mathbf{u}_i \mathbf{v}_i^T. \qquad (1.1.13)
$$

---

[6]The zero- and first-degree terms are omitted because both the bodies of the Earth and the reference ellipsoid are assumed to have the same mass and angular rotation velocities, and the origin of the geocentric coordinate system coincides with the common centre of mass for both bodies (Heiskanen and Moritz, 1967, sect. 2-18)

The other eigenvalue system for **B**:

$$(\mathbf{u}_i, \mathbf{v}_i^T; \lambda_i)_{i \leq n}, \qquad\qquad (1.1.14)$$

is a sequence of vectors, $\mathbf{u}_i$, $\mathbf{v}_i^T$, called left- and right-eigenvectors, and real/non-negative numbers λ_i, called eigenvalues, satisfying five properties (see Appendix A), where n denotes the dimensionality of the matrix. As usual, the transpose of an eigenvector is designated by the superscript T. For example, $\mathbf{v}_i^T$ represents the transpose of $\mathbf{v}_i$. For more definitions in depth, see Chapter 2.

Second, two eigenvalue systems can be associated with the so-called Molodenskij's modification scheme. It was Molodenskij in 1962 who first introduced the concept of truncating Stokes's integration domain and of modifying Stokes's integration kernel. For computational convenience, one only works in a selected area of interest integrated over a limited spherical cap instead of on the whole Earth. The deterministic modification of the Stokes's solution of the GBVP has been broadly investigated by many geodesists, e.g., de Witte (1967), Wong and Gore (1969), Meissl (1971a, 1971b), Paul (1973), Rapp and Rummel (1975), Jekeli (1981b), Wenzel (1982), Wichiencharoen (1984), Sjöberg (1984, 1986, 1991), Vaníček and Kleusberg (1987), Petrovskaya and Pischukhina. (1990), Vaníček *et al.* (1990), Vaníček and Sjöberg (1991), Smeets (1994), Vaníček and Featherstone (1998) and Featherstone *et al.* (1998). In this thesis, we focus on the DBVP for the HDC formulation using Molodenskij's modification scheme. Put forward and modified by Vaníček *et al.* (1996), the first kind Fredholm integral equation can be divided into two zones: the near zone and the far zone:

1. In the near zone contribution (NZC), the integral (Sun and Vaníček, Eq. (24) and (25), 1998) has the form:

$$\left(\Delta g^h(r_t, \Omega)\right)^L = \frac{R}{4\pi r_t} \int_{C_0} \left(\Delta g^h_{c:g}(\Omega')\right)^L \overline{K}^m(H^O, \psi, \psi_0) d\Omega', \qquad (1.1.15)$$

where C_0 denotes a spherical cap over the Earth:

$$\overline{K}^m(H^O, \psi, \psi_0) = K(H^O, \psi) - \sum_{j=0}^{L} \frac{2j+1}{2} t_j(H^O, \psi_0) P_j(\cos \psi) \qquad (1.1.16)$$

8

is the modified Poisson kernel with unknown coefficients t_j, which can be taken from (Sun and Vaníček, 1998), where $K(H^O, \psi)$ is the Poisson kernel (Vaníček *et al.*, Eq. (20), 1996), and the superscript index L is used to represent the high frequency part of the Helmert gravity anomaly that is related to the cut-off degree of the $\overline{K}^m$. Equation (1.1.15) is discretized giving a system of linear algebraic equations, i.e.:

$$\left(\Delta \mathbf{g_t^h}\right)^{\mathbf{L}} = \mathbf{B} \left(\Delta \mathbf{g_{c:g}^h}\right)^{\mathbf{L}}, \tag{1.1.17}$$

which is studied with emphasis on the conditioning of the non-symmetrical matrix $\mathbf{B} \in \mathbb{R}^{n \times n}$ arising from the discretized problem, where $\left(\Delta \mathbf{g_t^h}\right)^{\mathbf{L}} \in \mathbb{R}^{n \times 1}$ denotes an input (or known) vector of mean Helmert gravity anomalies on $\mathbb{H}_t$ with the length n and $\left(\Delta \mathbf{g_{c:g}^h}\right)^{\mathbf{L}} \in \mathbb{R}^{n \times 1}$ denotes an output (or unknown) vector of mean Helmert gravity anomalies on $\mathbb{H}_{c:g}$ with the length n. Using the DOWN97' package (written by Huang and Vaníček, 1997), our present belief is that the error as the difference between the exact solution and the approximate solution of the integral equation for constructing the matrix $\mathbf{B}$ is of sufficiently small. This coefficient matrix $\mathbf{B}$ only depends on the orthometric heights. A method for getting the eigenvectors of $\mathbf{B}$ viz the QEVD is important in connection with a discrete set of Helmert gravity anomalies in the Earth's topography within a spherical cap (the input data). A product of the eigenvectors and the input data (which can be considered as the Fourier coefficients) is defined as the *Helmert gravity anomaly coefficients* $\mathbf{u}_i^T \left(\Delta \mathbf{g_t^h}\right)^{\mathbf{L}} \in \mathbb{R}$.

2. In the far zone contribution, the integral has the form:

$$D_{\Delta g_t^h}(\Omega) = \frac{R}{4\pi r_t} \int_{\Omega' - C_0} D_{\Delta g_{c:g}^h}(\Omega') \overline{K}^m(H^O, \psi, \psi_0) d\Omega'. \tag{1.1.18}$$

Equation (1.1.18) can be expressed in its analytical form when two physical quanlities, $D_{\Delta g_t^h}$ and $D_{\Delta g_{c:g}^h}$, are expanded as the infinite series of harmonic

functions, given as the *truncation error* (TE) of the truncated Poisson integration in spectral form (Vaníček *et al.*, 1996) on the Earth's topography and on the Helmert co-geoid, respectively. In the spectral domain, the TE on the Helmert co-geoid can be represented by the cut-off series of harmonic functions when we use the existing geopotential models[7] as *á priori* information on the input. We propose that the derivation of the TE is similar to the one given by (ibid.) except it is slightly modified by the author, in the context of formulating the TE as an inverse problem instead of a direct problem. That is:

$$\epsilon g_{c:g}^h(\Omega') = \frac{GM}{R^2} \sum_{j=21}^{I_{\max}} (j-1) \frac{\left(\frac{R}{R+H^O}\right)^{j+1}}{\frac{\overline{Q}_j(H^O,\psi_0)}{2}} \sum_{m=-j}^{j} [T_t^h]_{jm} Y_{jm}(\Omega') \qquad (1.1.19)$$

(See Wong and Vaníček (2000) for a detailed derivation of Eq. (1.1.19)). The above expression is different from Vaníček *et al.* (in Appendix, Eq. (48), 1996) and Sun and Vaníček (Eq. (23), 1998), i.e.:

$$D_{g_T}(\Omega) = \frac{R\gamma}{2r} \sum_{j=21}^{I_{\max}} (j-1) \overline{Q}_j(H^O,\psi_0) \sum_{m=-j}^{j} T_{jm} Y_{jm}(\Omega) \qquad (1.1.20)$$

in that the coefficients $\overline{Q}_j(H^O, \psi_0)$ are in the denominator instead of the numerator. Using the existing geopotential models leads us to evaluating the Fourier coefficients of the TE, given as the *disturbing potential coefficients*[8]. From Equation (1.1.10), we can derive a discrete set of eigenvalues viz the EVE, referred to as a discrete set of the modified Molodenskij-Poisson coefficients.

---

[7]The global geopotential coefficients are given as a set of fully normalized gravitational coefficients $\{\forall\ j \geq 2,\ -j \leq m \leq +j :\ [W^g]_{jm} = (\overline{C}_{jm}, \overline{S}_{jm})\}$ of the Earth's surface, which are given in a two-dimensional Euclidean manifold of any well-suited sphere $\mathbb{S}^2$ that is valid only in the harmonic space (e.g., the Goddard Earth model (GEM)-Tn-series and the Joint Gravity Model (JGM)-n series (Marsh *et al.*, 1988; Lerch *et al.*, 1994; Nerem *et al.*, 1994; Tapley *et al.*, 1996), the GSFC/NIMA EGM96 model (Lemoine *et al.*, 1997), the GRIM-series models (Schwintzer *et al.*, 1997), the OSU models (Rapp *et al.*, 1991), the University of Texas Earth gravitational model (TEG)-series models (Tapley, *et al.*, 1996) and the ultra high degree geopotential models (GPM)-series model (Wenzel, 1998)).

[8]The Helmert disturbing coefficients $[T^h]_{jm}$ are not readily available. Proposed by Vaníček *et al.*, these coefficients can be estimated by one of the existing geopotential models as *á priori* information

We need to show that if the DPT is satisfied, interpreted as the sequence of the ratio, the Helmert gravity anomaly coefficients and the disturbing potential coefficients must decay to zero faster than two sets of eigenvalues with respect to the orthonormal system in the mean-square sense. Transformed the above sentence into the mathematical expression, we have two formulæ:

Near Zone Using the DPT in the solution of $\left(\Delta g_{c:g}^h\right)^L$, the *discrete Picard-Helmert coefficients* in the absolute sense:

$$\forall\, 1 \le i \le n: \quad \left| \mathbf{v}_i^T \left(\Delta \mathbf{g}_{\mathbf{c:g}}^{\mathbf{h}}\right)^{\mathbf{L}} \right| = \left| \frac{\mathbf{u}_i^T \left(\Delta \mathbf{g}_{\mathbf{t}}^{\mathbf{h}}\right)^{\mathbf{L}}}{\lambda_i} \right| \tag{1.1.23}$$

die off.

Far Zone Using the DPT in the solution of $D_{\Delta g_{c:g}^h}(\Omega')$, the truncation error coefficients in the absolute sense:

$$\forall\, 21 \le j \le I_{\max} \text{ and } -j \le m \le j: \quad \left| Y_{jm}^* D_{g_{c:g}^h} \right|_{(\Omega')} = \frac{GM}{R^2} \left| \frac{[T_t]_{jm}}{\varsigma_j} \right| \tag{1.1.24}$$

on the input. The disturbing potential coefficients are:

$$\forall\, 21 \le j \le I_{\max}: \quad \sum_{m=-j}^{j} [T_t^h]_{jm} \equiv \sum_{m=-j}^{j} [T_t]_{jm} = \left[[W^g]_{j0} - [U^g]_{j0} + \sum_{\substack{m=-j \\ m \neq 0}}^{j} [W^g]_{jm} \right]. \tag{1.1.21}$$

The global geopotential coefficients are given as a set of fully normalized gravitational coefficients $\{\forall\, j \ge 2,\ -j \le m \le +j:\ [W^g]_{jm} = (\overline{C}_{jm}, \overline{S}_{jm})\}$ of the Earth's surface, which are given in a two-dimensional Euclidean manifold of any well-suited sphere $\mathbb{S}^2$ that is valid only in the harmonic space. Given as a spectral representation of the normal gravitational potential U^g, a set of fully normalized normal gravitational potential coefficients $\{\forall j \ge 2,\ m = 0:\ [U^g]_{j0} = \overline{C}_{j0}^*\}$ of the chosen conventional reference ellipsoid has the form (Heiskanen and Moritz, 1967):

$$\forall j \ge 2,\ m = 0:\ [U^g]_{j0} = (-1)^{\frac{j}{2}+1} \frac{3e^j}{(j+1)(j+3)} \left(1 - 0.5j + 2.5j \frac{J_2}{e^2} \right), \tag{1.1.22}$$

where e is the first eccentricity, J_2 is the second degree coefficient, representing the flattening of the reference (normal) ellipsoid. The coefficients $\{\forall\, j \ge 2,\ m = 0:\ [U^g]_{j0} = \overline{C}_{j0}^*\}$ exist only for zonal degree coefficients due to the symmetric property with respect to the equatorial plane, and setting $m = 0$ due to the symmetric property with respect to the rotation z-axis. It is important to mention that the coefficients $[U^g]_{j0}$ decrease to zero for $j > 8$ (Vaníček and Kleusberg, 1987).

11

fade away, where $GM = 3.986 \times 10^{14} \mathrm{m}^3 \mathrm{s}^{-2}$ is the geocentric gravitational constant and ς_j denotes the eigenvalues of $D_{g_{c:g}^h}(\Omega')$, i.e.:

$$\forall \, 21 \leq j \leq I_{\max}: \qquad \varsigma_j = \frac{1}{j-1} \frac{\overline{Q}_j(\overline{\mathcal{H}}^O, \psi_0)}{2} \left(\frac{R}{R+H^O}\right)^{j+1}.$$

In this thesis, the focus is only on the case of the near zone contribution. In this regard, from Equation (1.1.23), we show that the stability and existence of a solution for the HDC in the NZC can be analyzed in spectral form using the discrete Picard technique. Moreover, the results obtained in this form are of interest by themselves, since they can be regarded as proof of the stable behaviour and the existence of the solution, leading to the well-posedness of the HDC in the NZC. Concerning the stability and existence of a solution for Equation (1.1.24), in the future the case of the far zone contribution and how the discrete Picard technique can be used will be addressed.

1.2 Outline of the Thesis

The thesis is organized as follows.

The theory of the existence, uniqueness, and stability of a solution for the linear Fredholm integral equation of the first kind for determining the Helmert gravity anomaly on the Helmert co-geoid is discussed in Chapter 2. The existence of a solution to the HDC problem in the NZC to be tested in Hadamard's sense leads to the construction of a framework of the QEVD. In Section 2.1, the original *singular value decomposition* (SVD) is slightly modified, to give the QEVD. Since on the main diagonal of a non-symmetric matrix $\mathbf{B}$ there is a finite set of the non-zero/non-negative eigenvalues, the QEVD is used instead of the SVD. This technique is then applied to the analysis of the finite spectral representation of the matrix-vector-valued function. The behaviour of the eigenvalues of $\mathbf{B}$ is studied. In the NZC, a discrete set of mean Helmert gravity anomalies is discussed and used.

In Chapter 3, we use the QEVD to formulate Picard's criterion in a compact and a discrete manner. To the best of the author's knowledge this is first time that the discrete Picard technique is used for analyzing the numerical behaviour of geopotential coefficients and Helmert gravity anomalies for the HDC viz QEVD. The well-posedness of the HDC problem can be justified by the numerical results of the DPT.

In Chapter 4, the final conclusions of this work and some suggestions for future work are given.

Chapter 2

Well-posed Problems of Harmonic Downward Continuation

According to Jacques Hadamard (who summarized a result from the work of Cauchy, Kowaleski, Darboux, Goursat and Holmgren), he suggested in 1902 that a problem is called "well-posed" if a solution (or an output) exists that is arbitrary (within a certain range), does not have more than one solution, and depends continuously on the input data. If one of the above-mentioned requirements fails, the problem is said to be "ill-posed".

Precisely corresponding point-by-point, to the definition of well-posedness of the HDC problem, we note the following remarks:

(a) "A unique solution" is equivalent to "all eigenvalues in the degenerate kernel (e.g., MMPTK) and the finite dimensional non-symmetric matrix are non-zero when the indices j and i are monotonically increasing" (e.g., Groetsch, 1993; Hansen, 1998).

(b) The solution of existence can be expounded by the Picard criterion (e.g., Wahba, 1973; Varah, 1973; Strand, 1974; Hansen, 1990).

(c) "The inverse is not continuous" is equivalent to "the inverse is unbounded" (e.g.,

Tikhonov, 1963, 1964). In other words, the inverse mapping from $\Delta g^h \in \mathbb{H}_t$ to $\Delta g^h \in \mathbb{H}_{c:g}$ through the linear Fredholm integral equation of the first kind is continuous.

The most common cause of an ill-posed problem in the HDC in the NZC may be due to the eigenvalues of the degenerate kernel and of the finite dimensional non-symmetric matrix. The faster the eigenvalues tend to zero, the more severe becomes the ill-posedness. In what follows, we study under what circumstances the eigenvalues of the finite dimensional non-symmetric matrix decay to zero.

2.1 Integrated Modified Poisson Kernel and Quasi-Eigenvalue Decomposition

The HDC problem can be solved using a system of linear algebraic equations with a discrete set of Helmert gravity anomaly values when the right-hand side of the integral (1.1.9) is discretized by means of the doubly averaged integration technique. Discretization of Eq. (1.1.9) is also performed using the Gaussian quadrature rules and Romberg integration, modification of Poisson kernel/spherical cap, and Lagrangian interpolation (Vaníček *et al.*, 1996).

As studied by Vaníček *et al.* (1996) and Sun and Vaníček (1997, 1998), in the $3° \times 5°$ block, discretization of Eq. (1.1.9) can be written in the matrix-vector form as:

$$\left(\Delta \mathbf{g_t^h}\right)^{\mathbf{L}} = \mathbf{B}\left(\Delta \mathbf{g_{c:g}^h}\right)^{\mathbf{L}}, \tag{2.1.1}$$

where $\mathbf{B}$ is the coefficient matrix (c.f., Eq. (1.1.12)). The calculation of the inversion matrix (i.e., $\mathbf{B}^{-1}$) can be determined using either the direct method or the iterative method. Direct methods compute the exact inversion matrix (i.e., $\mathbf{B}^{-1}$) after a finite number of steps. Iterative methods, on the other hand, not only produce the exact

inversion matrix after a finite number of steps but also gradually decrease the error by some fractions in each iteration until the desired accuracy level is reached. Neither methods, however, gives any information on how the solution of $\left(\Delta \mathbf{g_{c:g}^h}\right)^{\mathbf{L}}$ is affected by $\mathbf{B}^{-1}$. This explains why we need to use techniques for analyzing the behaviour of $\mathbf{B}$.

The other eigenvalue system for $\mathbf{B}$:

$$(\mathbf{u}_i, \mathbf{v}_i^T; \lambda_i)_{i \leq n}, \tag{2.1.2}$$

is a sequence of vectors, $\mathbf{u}_i, \mathbf{v}_i^T$, called left- and right-eigenvectors, and real/non-negative numbers λ_i, called eigenvalues, satisfying five properties (see Appendix A), where n denotes the dimensionality of the matrix. Similar to the definition of the Eigenvalue Decomposition (EVD) (e.g., Bjerhammar, 1973b; Golub and Van Loan, 1983; Ren, 1996), the non-symmetric matrix $\mathbf{B}$ can be written in a spectral vector-form[1] as:

$$\mathbf{B} = \sum_{i=1}^{n} \lambda_i \mathbf{u}_i \mathbf{v}_i^T \tag{2.1.3}$$

which is called the Quasi-Eigenvalue Decomposition (QEVD) of $\mathbf{B}$. The term "Quasi" has one meaning which comes from the product of $\mathbf{u}_i$ and $\mathbf{v}_i^T$ which is not equivalent to the identity vector $\mathbf{I}$ (i.e., $\sum_{i=1}^{n} \mathbf{u}_i \mathbf{v}_i^T \neq \mathbf{I}$).

The analogy between the singular value decomposition (SVD[2]) of a matrix $\mathbf{B}$ and the QEVD has the same LINPACK[3] (Dongarra *et al.*, 1979) library of Fortran routines for solving the linear systems of equations, eigenvalues and eigenvectors. For the numerical computations and graphical representations, the LINPACK-based numerics library incorportated with the computer software package MATLAB is used.

---

[1] $\mathbf{B} = \sum_{i=1}^{n} \lambda_i \mathbf{u}_i \mathbf{v}_i^T \equiv \sum_{i=1}^{n} \mathbf{u}_i \lambda_i \mathbf{v}_i^T$.

[2] The example of the SVD on use of geodetic applications is widely used by Rummel, Schwarz and Gerstl (1979), and Ilk (1987, 1993). The numerical example of the ill-conditioned systems from observation data is studied by Branham (1979, 1980).

[3] The name LINPACK is an acronym for Linear Algebra PACKage.

In constrast with the SVD, the diagonal elements of $\mathbf{B}$ only contains a set of non-zero/non-negative eigenvalues. The QEVD of any square real matrix $\mathbf{B}$ is said to be simultaneously diagonalizable if

$$\mathbf{B} = \mathbf{U}\Lambda\mathbf{V^T}, \tag{2.1.4}$$

where $\mathbf{U}$ and $\mathbf{V^T}$ are orthogonal matrices (i.e., $\mathbf{UU^T} = \mathbf{I}$, and $\mathbf{V^TV} = \mathbf{I}$, and $\mathbf{UV^T} \neq \mathbf{I}$), and Λ is a diagonal matrix with the eigenvalues. More succinctly, one gets:

$$
\begin{aligned}
\Lambda &= \text{Diag}(\lambda_1, \cdots, \lambda_n) \in \mathbb{R}^{n \times n} \\
\mathbf{U} &= [\mathbf{u}_1 \ \mathbf{u}_2 \ \cdots \ \mathbf{u}_n] \in \mathbb{R}^{n \times n} \\
\mathbf{V} &= [\mathbf{v}_1 \ \mathbf{v}_2 \ \cdots \ \mathbf{v}_n] \in \mathbb{R}^{n \times n}.
\end{aligned}
$$

In general, two consequences of the non-symmetric matrix $\mathbf{B}$ associated with the band-structure of diagonal elements are:

1. If the matrix $\mathbf{B}$ acts as a smoothing operator, the eigenvalues λ_n of the discrete/square matrix will automatically decay rapidly to zero. The direct solution of Helmert gravity anomaly vectors $\left(\Delta \mathbf{g_{c:g}^h}\right)^{\mathbf{L}}$ dampens the oscillating variation of $\left(\Delta \mathbf{g_t^h}\right)^{\mathbf{L}}$ and result in a loss of information because of the smoothing effects.

2. In contrast with the direct problem, if one tries to recover $\left(\Delta \mathbf{g_{c:g}^h}\right)^{\mathbf{L}}$, the matrix must be inverted and transformed to the right-hand side. Due to this mathematical operation, the inverse problem amplifies the final product $\left(\Delta \mathbf{g_{c:g}^h}\right)^{\mathbf{L}}$ enhancing the high-frequency behaviour. The expected amplification comes from the eigenvalues of $\mathbf{B}$ (which depends on the orthometric heights). If some orthometric height data points are too close together or too far away from the Earth's surface, the matrix $\mathbf{B}$ automatically causes the resultant solutions of $\left(\Delta \mathbf{g_{c:g}^h}\right)^{\mathbf{L}}$ on $\mathbb{H}_{c:g}$ to be unstable since the inverse of $\mathbf{B}$ acts as an amplifying operator and may become numerically singular.

2.2 Mean Helmert Gravity Anomaly on the Earth's Topography

In the Helmert space setting, an observed Helmert gravity is $g^h(r_t, \Omega) = |gradW^h|_{(r_t,\Omega)}$, $W^h \equiv W_0 \in \Gamma_t$, where W^h is a Helmert gravity potential and Γ_t stands for the Earth's topography. The direction of $\mathbf{g}^h(r_t, \Omega)$ is perpendicular to the equipotential surfaces $W^h \equiv W_0$. As well a reference normal gravity is $\gamma([r_t - Z^h(r_t, \Omega)], \Omega) = |gradU|_{([r_t-Z^h(r_t,\Omega)],\Omega)}$, $U \equiv W_0 \in \Gamma_e$, where Γ_e stands for the region of the reference ellipsoid of revolution, $Z^h(r_t, \Omega)$ denotes the vertical displacement of the corresponding equipotential surfaces belonging to the two gravities. The direction of $\gamma([r_t - Z^h(r_t, \Omega)], \Omega)$ is perpendicular to the equipotential surfaces $U \equiv W_0$. Hence, a Helmert gravity anomaly $\Delta g^h(r_t, \Omega) \in \mathbb{H}_t$ is defined as the difference between the magnitudes $g^h(r_t, \Omega)$ and $\gamma([r_t - Z^h(r_t, \Omega)], \Omega)$. For a more definition in depth, see Vaníček et $al.$ (1999) and see Appendix B.

Collected terrestrial gravity data have an irregular pattern. The scatter over the land is much more dense than over sea. In order to transform the irregular pattern of terrestrial gravity data into a format of constituents blocks, one needs to generate an evenly spaced model over the surface of the global coverage for the advantage of doing fast and easy numerical computation. Moreover, one has to decompose the surface of the Earth into a number of discrete cells, which are classified by different pairs of co-latitudes and longitudes along different angular geographical grids from south to north in the meridian direction and from east to west in the prime vertical direction. Embraced by the curved trapezoid shape of the geographical grid, terrestrial gravity data points can be treated as either $point$ or $mean$ values. In this thesis, a discrete set of mean Helmert gravity anomalies is used.

Treated as input data, the high frequency component of the gravity field may be

described by the *mean Helmert gravity anomalies*:

$$\forall \, \Omega_i \in 3° \times 5° : \quad \overline{\left(\Delta g^h(R + H^O(\Omega_i), \Omega_i)\right)^L}$$

$$:= \operatorname*{mean}_{5' \times 5'}[\Delta g^{CB}(\Omega_i) + 2\pi\varrho_0 G H^O(\Omega_i) + \frac{2}{R}H^O(\Omega_i)\Delta g^{SB}(\Omega_i)$$

$$+ \delta\mathcal{I}^t(R + H^O(\Omega_i), \Omega_i) + \delta\mathcal{I}^a(R + H^O(\Omega_i), \Omega_i)$$

$$+ \delta\mathcal{A}^a(R + H^O(\Omega_i), \Omega_i) + \delta\mathcal{A}^{cr}(R + H^O(\Omega_i), \Omega_i)],$$

(2.2.5)

where Ω_i denotes the different geocentric angles within the $3° \times 5°$ block. It is important to note that $\operatorname{mean}_{5' \times 5'}[\cdot]$ stands for the mean Helmert gravity anomaly[4] taken from the mean value in regard to each grid-cell. Some fundamental concepts of mean Helmert gravity anomalies are provided in Appendix B or Vaníček *et al.* (1999). Numerical results for each component inside the square bracket can be found in (ibid.).

---

[4]The finite set of functional values $\{\overline{(\Delta g^h(R + H^O(\Omega_i), \Omega_i))^L}\}$ is not necessarily located at the centroid of the corresponding grid-cell, but it can be located anywhere within the grid-cell.

Chapter 3

Picard's Criterion

From the earlier discussion in Chapter 1.1 we have some indication of how to determine the existence of the solutions of $\Delta g^h \in \mathbb{H}_{\text{c:g}}$ by Picard's criterion under $\mathcal{L}^2$-norm estimations (see Appendix C) that we might propose. In Section 3.1 we state but do not proof the two theorems of the Picard criterion and discuss its application to the existence of the solution for the HDC. Section 3.2 will give details on different examples of numerical demonstrations in a real-life application.

3.1 Definition And Necessary Condition

This section contains important theorems in the development of the solution to the DBVP for the HDC, known as the Picard criterion. The Picard criterion can be divided into two cases: compact and discrete. They are the seeds for further discussions of practical computation. They are used and analyzed extensively for the linear Fredholm integral equation of the first kind (e.g., Hansen, 1990, 1998).

3.1.1 A Short Note of the Picard Criterion

Even though the French mathematician Picard (1910) was slightly influenced by the German mathematician Schmidt (1907) and the Hungarian mathematician Riesz when looking for the existence of a solution to the linear Fredholm integral equation of the first kind, he deserves credit as being the father of Picard's criterion. It was Picard himself who demonstrated the necessary condition for the first time, thus producing a context in which the Fourier coefficients must decay to zero faster than the eigenvalues with respect to the orthonormal system in the mean-square sense. Similar to Picard's formulation with a symmetric kernel, in 1937, the British mathematician Smithies reformulated the Picard criterion by means of the eigenfunction-eigenvalue analysis, but strongly emphasized the reference to singular values of the integral equation in our modern sense of the nomenclature rather than the eigenvalues. The singular values are referred to as a set of real, non-negative, non-zero and zero numbers, while the eigenvalues are referred to as a set of real and non-zero numbers only.

In Picard's paper, one recognizes that the eigenvalues of the kernel (as singular values) are in the numerator instead of the denominator. In other similar usage of Picard's criterion, the British mathematician Bateman (1908) refers to real numbers that are the reciprocals of the eigenvalues of the kernel as singular values. Here, we will adopt Picard's formulation when using the eigenvalue analysis. Moreover, an advantage of this expression is that it is closely related to matrix algebra. For more historical information, the well-written papers by Stewart (1993) and Kalman (1996) are strongly recommended.

3.1.2 Compact and Discrete Picard criterion

The original form of the Picard criterion is given below.

Theorem 1 *Compact Picard criterion (CPC) (Picard, 1909; Smithies, 1965). Let $(u_n, v_n; \nu_n)$ be a singular system of the $\mathcal{L}^2$ kernel $K(s, t)$, and let $g(s)$ be a given $\mathcal{L}^2$*

21

function. Then the equation

$$g(s) = \int K(s,t)f(t)dt \tag{3.1.1}$$

has an $\mathcal{L}^2$ solution $f(t)$ if and only if

(a) $\sum_{n=1}^{\infty} \left| \frac{(g,u_n)}{\nu_n} \right|^2 < +\infty,$

(b) $(g,u) = 0$ *for every $\mathcal{L}^2$ function u such that $K^*u = 0$ (Homegenity).*

Under these conditions a solution f of Eq. $Kf = g$ can be written as

$$\lim_{N \to \infty} f_N, \tag{3.1.2}$$

where

$$f_N = \sum_{n=1}^{N} \frac{(g,u_n)}{\nu_n}v_n. \tag{3.1.3}$$

For practical purposes, we will consider the following form of the compact Picard criterion instead.

Theorem 2 *Discrete Picard criterion (DPC) (Varah, 1973; Strand, 1974; Hansen, 1990). Let g denote the unperturbed right-hand side in Eq. (3.1.1). Then g satisfies the DPT if for all non-zero eigenvalues $\nu_n > eps$ the corresponding Fourier coefficients $|(g,u_n)|$, on the average, decay to zero faster than the ν_n, where eps stands for the floating-point relative accuracy. For computer machine precision[1] with IEEE floating-point arithmetic, $eps = 2^{-52}$, which is roughly $eps = 2.22e - 16$.*

In spite of all the efforts devoted to seeking out the existence of a solvable solution to the HDC problem, the compact and discrete Picard criterion has still its difficulties. Limitations arising from the definition of the CPC and DPC result in a necessary condition, but not a sufficient condition (Bitsadze, 1995).

---

[1]Also called machine unit roundoff or machine epilson

As mentioned earlier, the compact or discrete Picard criterion is a technique that indicates whether the sequence of the ratio converges or diverges. Regardless of which of the two definitions might be considered easier to use in a real-life situation, the basic problem right now is to demonstrate two different definitions for the same concept associated with the discrete Picard technique of the HDC. We therefore gather together the facts given about the QEVD in Chapter 2.

3.1.3   QEVD

Using the $5' \times 5'$ mean Helmert gravity anomaly in the $3° \times 5°$ block, the dimension of matrix $\mathbf{B}$ is 2160×2160. The matrix $\mathbf{B}$ not only depends on the orthometric heights, but it also lies at the heart of the different geocentric angles Ω_i within the spherical cap ψ_0. If $\left(\Delta \mathbf{g_t^h}\right)^{\mathbf{L}}$ also satisfies the Picard criterion, then a spectral representation (or an outer product expansion[2]) of the linear system of algebraic equations to the doubly averaged modified Poisson kernel is given by:

$$\left(\Delta \mathbf{g_{c:g}^h}\right)^{\mathbf{L}} = \mathbf{U}\Lambda^+\mathbf{V^T}\left(\Delta \mathbf{g_t^h}\right)^{\mathbf{L}} = \sum_{i=1}^{n} \frac{\mathbf{u}_i^T\left(\Delta \mathbf{g_t^h}\right)^{\mathbf{L}}}{\lambda_i}\mathbf{v}_i, \qquad (3.1.4)$$

where

$$\Lambda^+ = \mathrm{Diag}(\lambda_1^{-1}, \lambda_2^{-1}, \cdots, \lambda_n^{-1}), \qquad (3.1.5)$$

and

$$\left(\Delta \mathbf{g_t^h}\right)^{\mathbf{L}} = \overline{((\Delta g_t^h(R + H^O(\Omega_1), \Omega_1))^L}, \overline{(\Delta g_t^h(R + H^O(\Omega_2), \Omega_2))^L},$$
$$\cdots, \overline{(\Delta g_t^h(R + H^O(\Omega_n), \Omega_n))^L}), \qquad (3.1.6)$$

and $\mathbf{u}_i^T\left(\Delta \mathbf{g_t^h}\right)^{\mathbf{L}}$ denotes the Helmert gravity anomaly coefficients[3].

In the following section, we have two main goals. First, our aim is to demonstrate that absolute values of Helmert anomaly coefficients $\left|\mathbf{u}_i^T\left(\Delta \mathbf{g_t^h}\right)^{\mathbf{L}}\right|$ decay faster than

---

[2]This formula is similar to the Fourier series in the 1-D sense.

[3]The Helmert gravity anomaly coefficients are similar to the Fourier coefficients.

λ_i. Under this condition, we conclude that the existence of a solution for the HDC problem in the NZC valids. Using the DPT in the solution of $\left(\Delta\mathbf{g}_{\mathbf{c:g}}^{\mathbf{h}}\right)^{\mathbf{L}}$, the discrete Picard-Helmert coefficients in the absolute sense are defined as:

$$\forall\ 1 \leq i \leq n: \quad \left|\mathbf{v}_i^T\left(\Delta\mathbf{g}_{\mathbf{c:g}}^{\mathbf{h}}\right)^{\mathbf{L}}\right| = \left|\frac{\mathbf{u}_i^T\left(\Delta\mathbf{g}_{\mathbf{t}}^{\mathbf{h}}\right)^{\mathbf{L}}}{\lambda_i}\right|. \tag{3.1.7}$$

Second, numerical results validating the finite sets of $\left|\mathbf{u}_i^T\left(\Delta\mathbf{g}_{\mathbf{t}}^{\mathbf{h}}\right)^{\mathbf{L}}\right| \in \mathbb{R}$ and $\left|\frac{\mathbf{u}_i^T\left(\Delta\mathbf{g}_{\mathbf{t}}^{\mathbf{h}}\right)^{\mathbf{L}}}{\lambda_i}\right| \in \mathbb{R}$ can be measured their differences due to the variations of eigenvalues. These comparison are very useful in determining the stability of a solution for the HDC problem in the NZC.

3.2 Applications and Recommentations

As outlined by Sjöberg (1979) and discussed by Martinec (1996), and also according to the necessary condition of the compact Picard criterion, if Equation (1.1.9) has a solvable solution, then the expression of Equation (3.1.7), must converge in the $\mathcal{L}^2$-norm where there exists a set of infinitely many eigenvalues. However, the ideal of the infinite or compact case is only of theoretical interest (e.g., Engl (1981)).

The burning question now is: Why do we need to study the technique of Picard's criterion? It is because Picard's criterion intervened with the following two observed functionals, namely, of which the first seems to reveal how the behaviour of a *Helmert gravity anomaly* navigating through the harmonic space outside the geoid is collected from the surface of the Earth, but then the second sheds light on an *orthometric height* by means of spirit levelling. Two physical quantities of this estimate would be expected to depend on the finite set of data. Hence, the discrete Picard technique can be made by simply taking the finite dimension of the matrix i. To see how the discrete Picard technique works, it will be useful to plot the graph in a spectral sense.

3.2.1   Analysis of the QEVD

For numerical illustrations, the following three $3° \times 5°$ areas of coverage of the mean Helmert gravity data are used; I: ($49°05'00'' \le \varphi \le 52°05'00''$ N, $239°05'00'' \le \lambda \le 243°55'00''$ E), II: ($47°05'00'' \le \varphi \le 50°05'00''$ N, $241°05'00'' \le \lambda \le 245°55'00''$ E), and III: ($46°05'00'' \le \varphi \le 49°05'00''$ N, $242°05'00'' \le \lambda \le 246°55'00''$ E).

Regional Area	Matrix $\mathbf{B}_{2160 \times 2160}$	$\lambda_{\max}$	$\lambda_{\min}$	Condition Number $\lambda_{\max}/\lambda_{\min}$
$49°05'00'' \le \varphi \le 52°05'00''$ $239°05'00'' \le \lambda \le 243°55'00''$	$\mathbf{B}_I$	1.2874	0.2286	5.6307
$47°05'00'' \le \varphi \le 50°05'00''$ $241°05'00'' \le \lambda \le 245°55'00''$	$\mathbf{B}_{II}$	0.9748	0.1796	5.4264
$46°05'00'' \le \varphi \le 49°05'00''$ $242°05'00'' \le \lambda \le 246°55'00''$	$\mathbf{B}_{III}$	0.9936	0.1768	5.6190

Table 3.1: Condition Numbers.

Since each $\mathbf{B}_{\{I,II,III\}}$ matrix is square and of full rank, the QEVD technique guarantees that a unique solution exists. It is therefore feasible to examine the behaviour of $\mathbf{B}_{\{I,II,III\}}$. Ill-conditioning has been regarded as a plague on numerical matrix methods. This problem may arise, for example, if

(a) the determinant of the coefficients of the matrix $\mathbf{B}_{\{I,II,III\}}$ is almost zero[4], or

(b) the coefficients themselves are in error that the matrix $\mathbf{B}_{\{I,II,III\}}$ contains a few blunder value, or

(c) the size of the matrix $\mathbf{B}_{\{I,II,III\}}$ is large.

---

[4]We find, from the applied numerical linear algebra (e.g., Demmel(1997)), that if $\det \left| \mathbf{B}_{\{I,II,III\}} \right| = 0$ then there are either an infinite number or no solutions of $\mathbf{B}^{-1} \left(\Delta \mathbf{g_t^h} \right)^{\mathbf{L}} = \left(\Delta \mathbf{g_{c:g}^h} \right)^{\mathbf{L}}$.

For a case with a large matrix $\mathbf{B}_{\{I,II,III\}}$, the condition number of $\mathbf{B}_{\{I,II,III\}}$ provides a measure of the degree of ill-conditioning; it is defined as the ratio of the largest eigenvalue to the smallest (e.g., Wing, 1985, 1992). The larger the condition number the greater the ill-conditioning. The eigenvalues of each matrix $\mathbf{B}_{\{I,II,III\}}$ in the selected areas of interest in Canada produced by the QEVD are plotted in Figs. 3.1(b), 3.5(b) and 3.9(b). Not surprisingly the results, which are listed in Table 3.1, are well-conditioned in concert with the numerical values of condition numbers. However, the disadvantage of the QEVD is the need for unrealistic time consumption when the dimensionality of the matrix is concerned.

Figures 3.1, 3.5 and 3.9 are called the *discrete Picard plot*. Each plot is composed of three graphs. They are:

1. Figures 3.1(a), 3.5(a) and 3.9(a) describe how the spectra of $\left| \mathbf{u}_i^T \left(\Delta \mathbf{g_t^h} \right)^{\mathbf{L}} \right|$ vary against the dimension of the diagonal matrices $\mathbf{B}_{\{I,II,III\}}$,

2. The eigenvalues λ_i of each matrix $\mathbf{B}_{\{I,II,III\}}$ against the dimension of the diagonal matrices are shown in Figs. 3.1(b), 3.5(b) and 3.9(b), and

3. Similarly, the spectra of $\left| \frac{\mathbf{u}_i^T \left(\Delta \mathbf{g_t^h} \right)^{\mathbf{L}}}{\lambda_i} \right|$ are shown in Figs. 3.1(c), 3.5(c) and 3.9(c) for demonstrating the sequences of ratios of $\left| \mathbf{u}_i^T \left(\Delta \mathbf{g_t^h} \right)^{\mathbf{L}} \right|$ and λ_i.

Comparison among Figures 3.1(a), 3.5(a) and 3.9(a) and 3.1(c), 3.5(c) and 3.9(c) indicate that the spectra of these coefficients are slightly magnified because of the inverse of the eigenvalues. Moreover, the discrete Picard technique demonstrates that each discrete Picard plot with respect to each $\mathbf{B}_{\{I,II,III\}}$ is not necessarily stable since the magnitude of these two coefficients, $\left| \mathbf{u}_i^T \left(\Delta \mathbf{g_t^h} \right)^{\mathbf{L}} \right|$ and $\left| \frac{\mathbf{u}_i^T \left(\Delta \mathbf{g_t^h} \right)^{\mathbf{L}}}{\lambda_i} \right|$, may vary significant. For example, Figure 3.1(c) has a wiggly characteristic pattern for its coefficient spectrum when the dimensionality of $\mathbf{B}_I$ increases. Inspection of Fig. 3.1(c) demonstrates that the trend of the coefficient spectrum goes up mildly when the eigenvalues of $\mathbf{B}_I$ rapidly decay after $i = 1500$. After operating the DPT, we see that

26

the small amplification of these coefficients mainly arising from the so-call *boundary effect* gives rise to an unstable situation. Our present belief is that the existence and stability of a solution for the HDC in the NZC could be analyzed in a spectral form, using DPT.
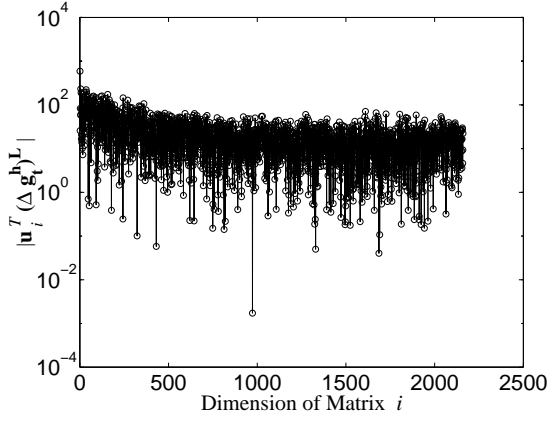
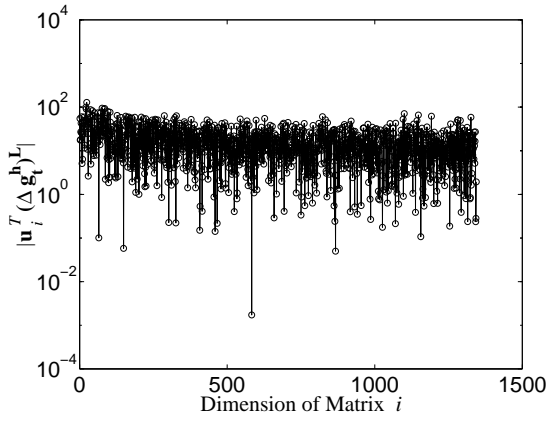(a) Helmert gravity anomaly coefficients $\left| \mathbf{u}_i^T \left(\Delta \mathbf{g}_t^h \right)^{\mathbf{L}} \right|$
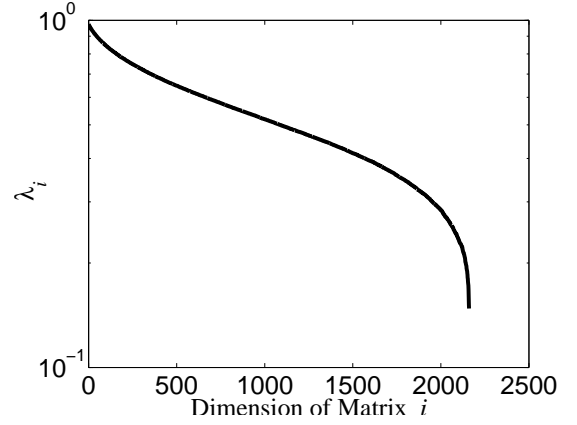
(b) The numerical eigenvalues λ_i of the 2160 × 2160 matrix $\mathbf{B}_I$
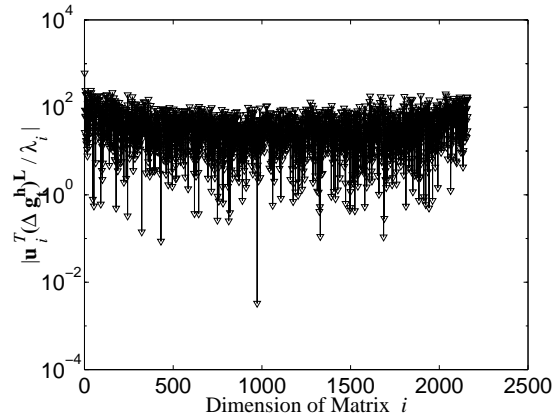
(c) Discrete Picard-Helmert coefficients $\left| \mathbf{u}_i^T \left(\Delta \mathbf{g}_t^h \right)^{\mathbf{L}} \right| / \lambda_i$
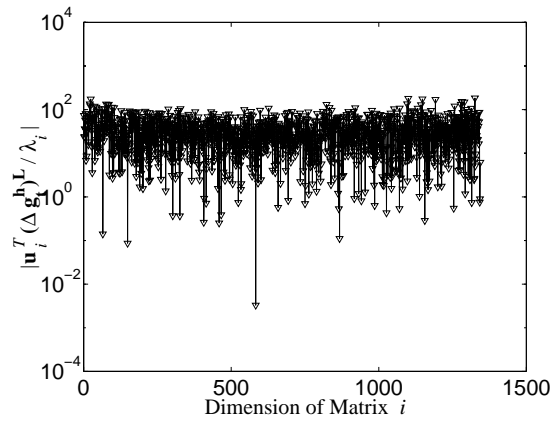
Figure 3.1: Discrete Picard plot of $\mathbf{B}_I$ in the 3° × 5° block.

(a) Helmert gravity anomaly coefficients $\left| \mathbf{u}_i^T \left(\Delta \mathbf{g_t^h} \right)^{\mathbf{L}} \right|$
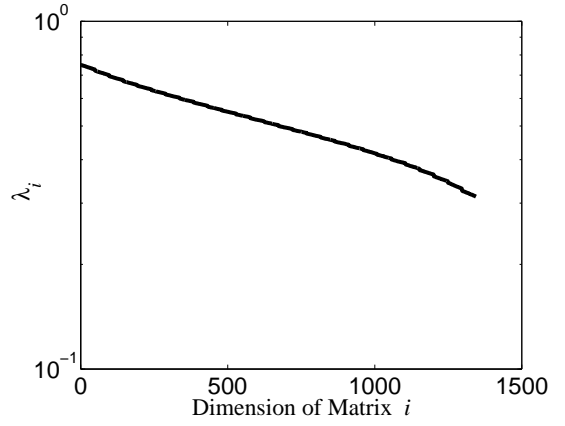
(b) The numerical eigenvalues λ_i of the 1152×1152 matrix $\mathbf{B}_I$

(c) Discrete Picard-Helmert coefficients $\left| \mathbf{u}_i^T \left(\Delta \mathbf{g_t^h} \right)^{\mathbf{L}} \right| / \lambda_i$

Figure 3.2: Discrete Picard plot of $\mathbf{B}_I$ in the $2° \times 4°$ block.

Figure 3.3: A comparison plot of discrete Picard-Helmert coefficients and Helmert gravity anomaly coefficients in the $3° \times 5°$ block of $\mathbf{B}_I$ (in mGal).
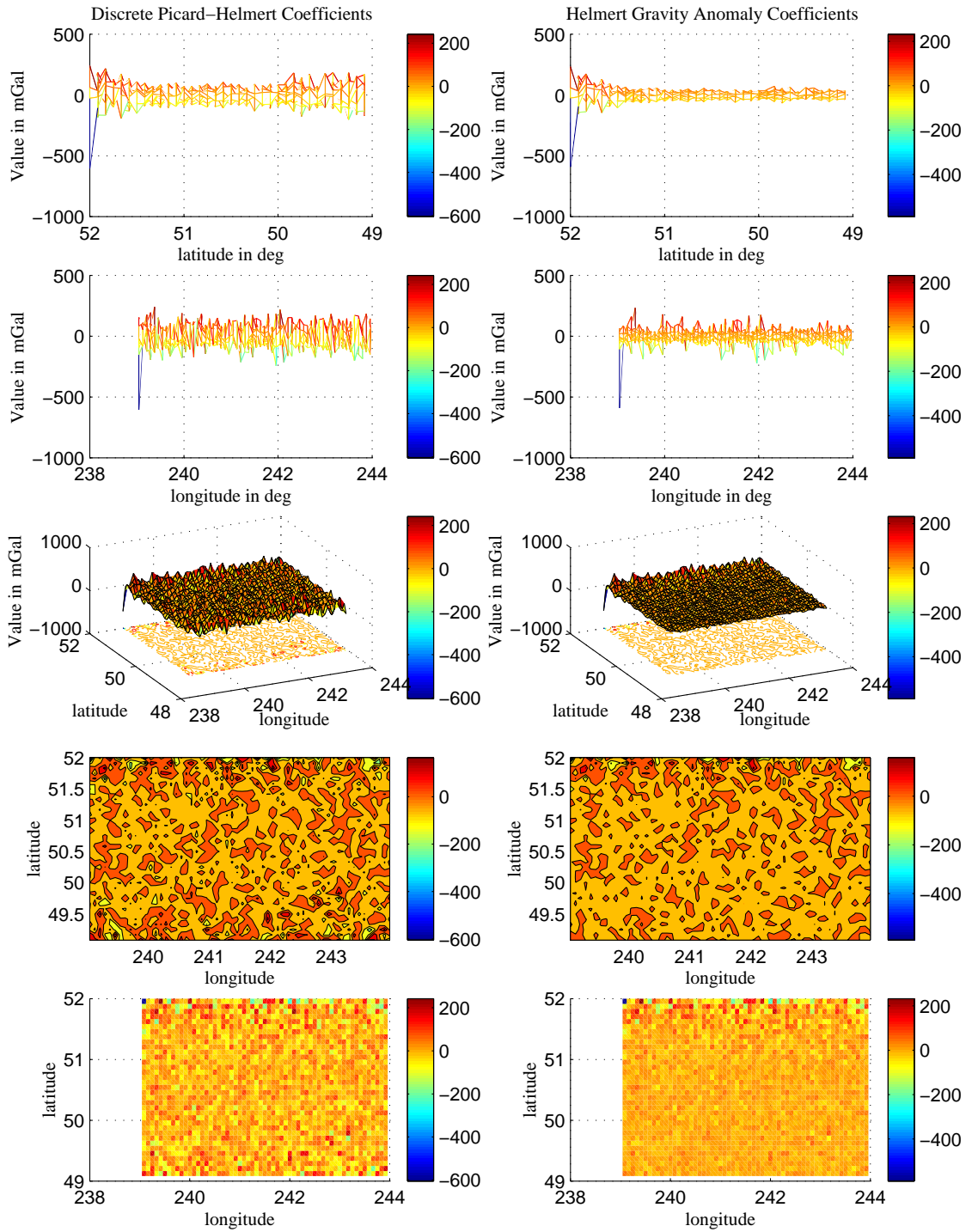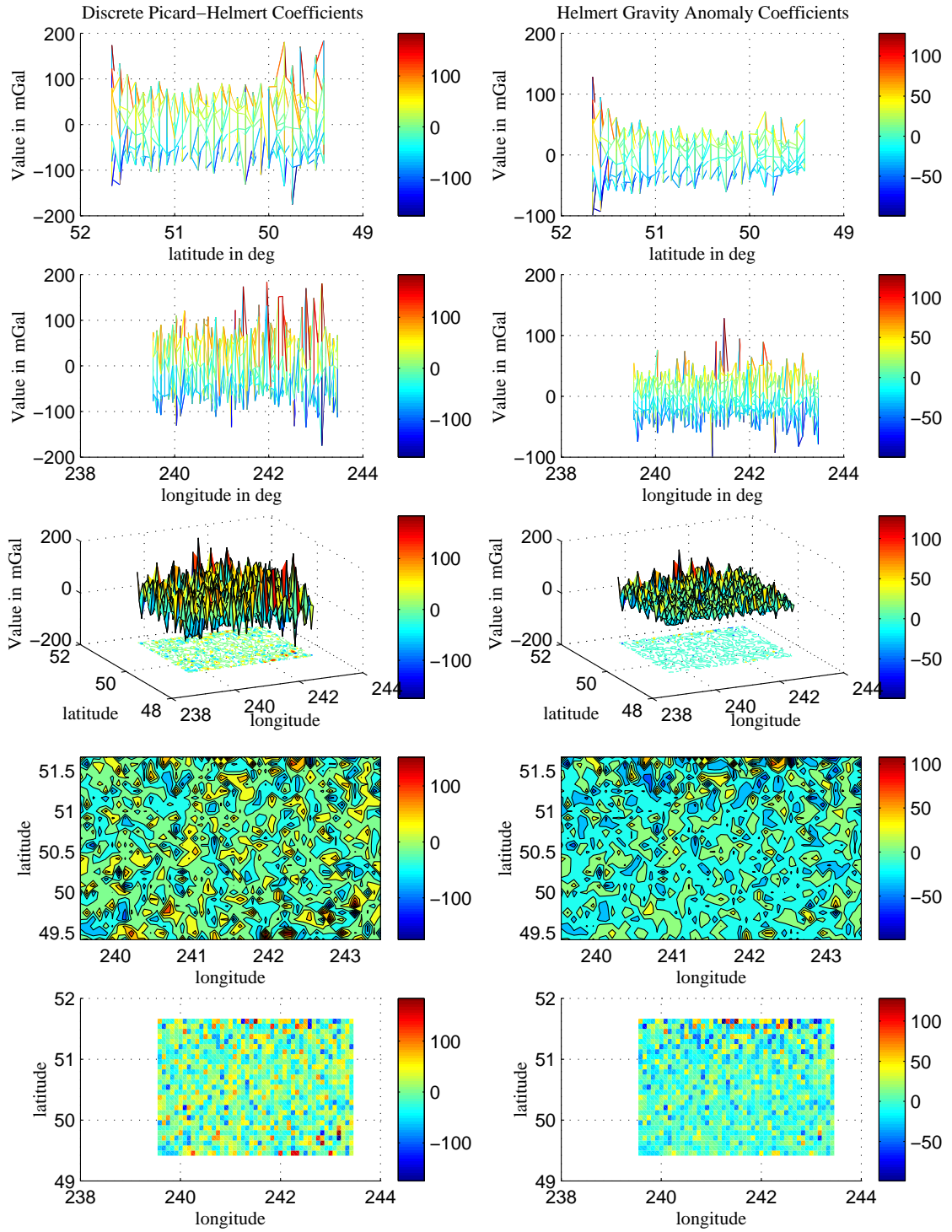
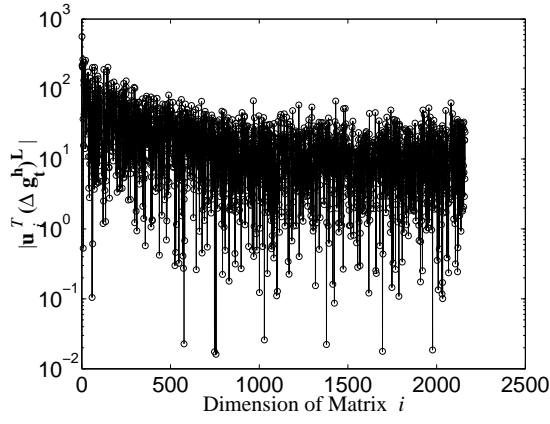Figure 3.4: A comparison plot of discrete Picard-Helmert coefficients and Helmert gravity anomaly coefficients in the $2° \times 4°$ block of $\mathbf{B}_I$ (in mGal).

(a) Helmert gravity anomaly coefficients $\left| \mathbf{u}_i^T \left(\Delta \mathbf{g_t^h} \right)^{\mathbf{L}} \right|$

(b) The numerical eigenvalues λ_i of the 2160 × 2160 matrix $\mathbf{B}_{II}$

(c) Discrete Picard-Helmert coefficients $\left| \mathbf{u}_i^T \left(\Delta \mathbf{g_t^h} \right)^{\mathbf{L}} \right| / \lambda_i$

Figure 3.5: Discrete Picard plot of $\mathbf{B}_{II}$ in the $3° \times 5°$ block.

(a) Helmert gravity anomaly coefficients $\left| \mathbf{u}_i^T \left(\Delta \mathbf{g_t^h} \right)^{\mathbf{L}} \right|$
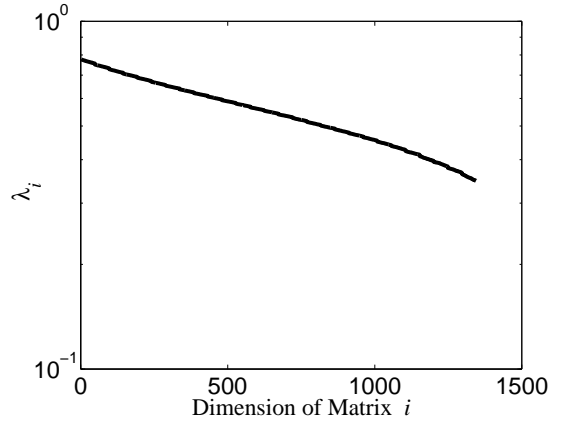
(b) The numerical eigenvalues λ_i of the 1152×1152 matrix $\mathbf{B}_{II}$

(c) Discrete Picard-Helmert coefficients $\left| \mathbf{u}_i^T \left(\Delta \mathbf{g_t^h} \right)^{\mathbf{L}} \right| / \lambda_i$

Figure 3.6: Discrete Picard plot of $\mathbf{B}_{II}$ in the $2° \times 4°$ block.

Figure 3.7: A comparison plot of discrete Picard-Helmert coefficients and Helmert gravity anomaly coefficients in the $3° \times 5°$ block of $\mathbf{B}_{II}$ (in mGal).
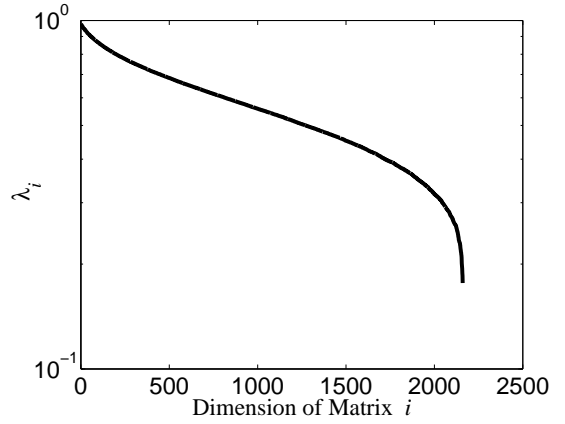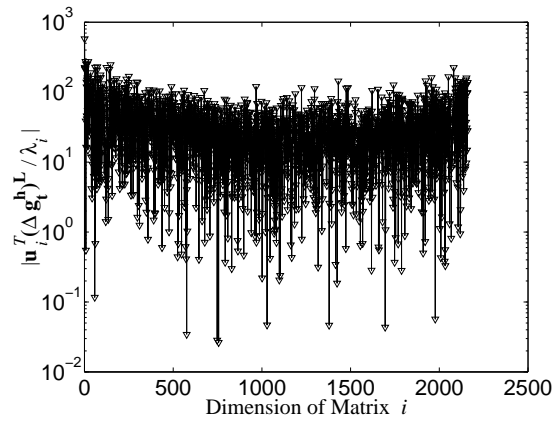
Figure 3.8: A comparison plot of discrete Picard-Helmert coefficients and Helmert gravity anomaly coefficients in the $2° \times 4°$ block of $\mathbf{B}_{II}$ (in mGal).
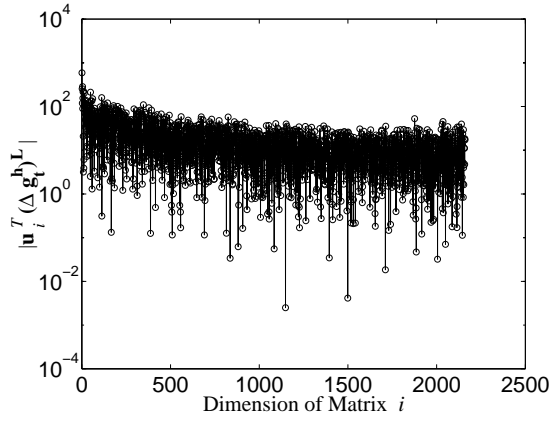
(a) Helmert gravity anomaly coefficients $\left| \mathbf{u}_i^T \left(\Delta \mathbf{g_t^h} \right)^{\mathbf{L}} \right|$
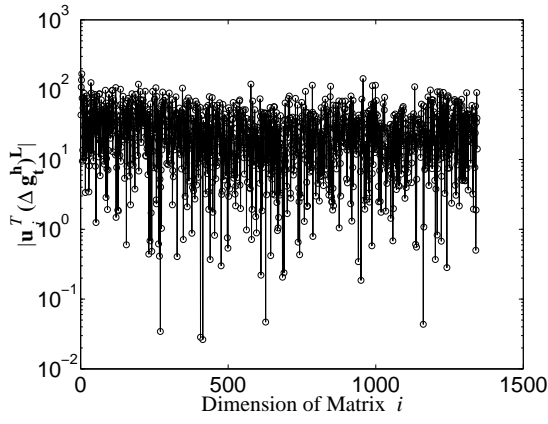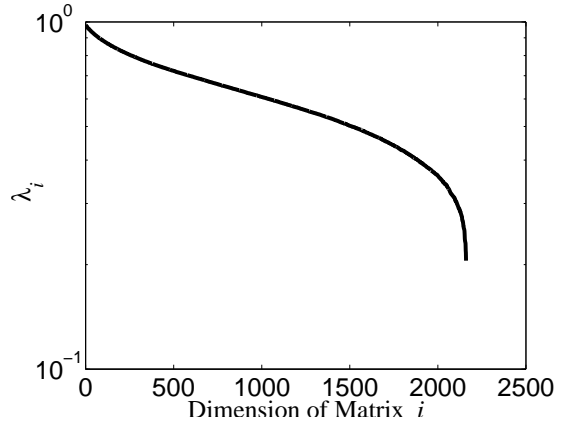
(b) The numerical eigenvalues λ_i of the 2160 × 2160 matrix $\mathbf{B}_{III}$

(c) Discrete Picard-Helmert coefficients $\left| \mathbf{u}_i^T \left(\Delta \mathbf{g_t^h} \right)^{\mathbf{L}} \right| / \lambda_i$
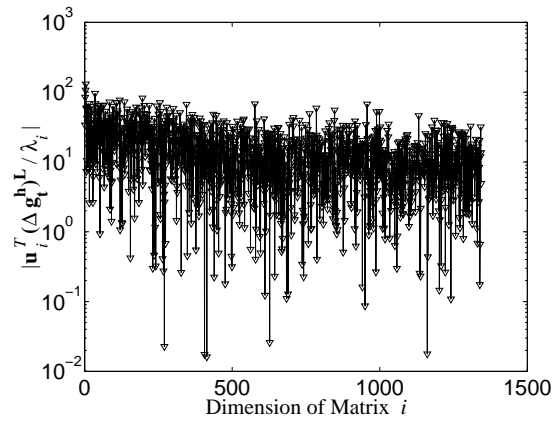
Figure 3.9: Discrete Picard plot of $\mathbf{B}_{III}$ in the $3° \times 5°$ block.
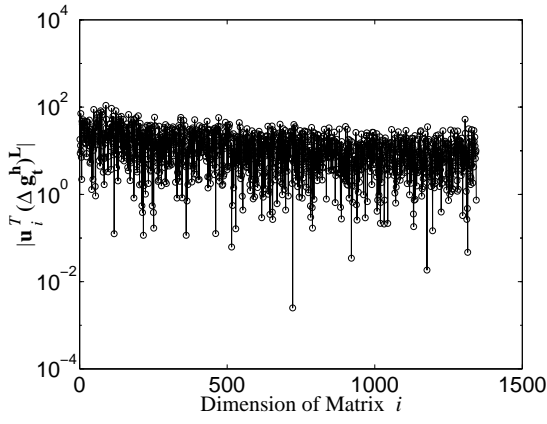
(a) Helmert gravity anomaly coefficients $\left| \mathbf{u}_i^T \left(\Delta \mathbf{g_t^h} \right)^{\mathbf{L}} \right|$
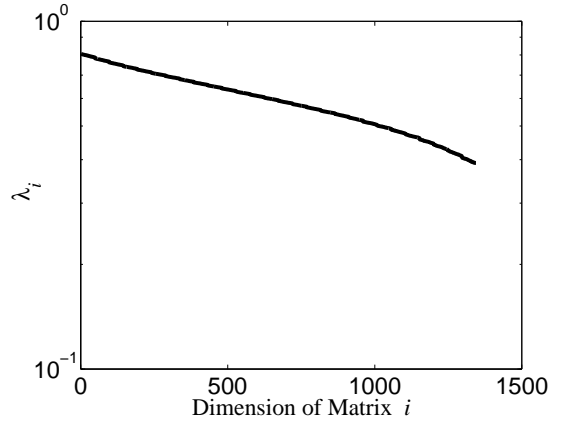
(b) The numerical eigenvalues λ_i of the 1152 $\times$ 1152 matrix $\mathbf{B}_{III}$
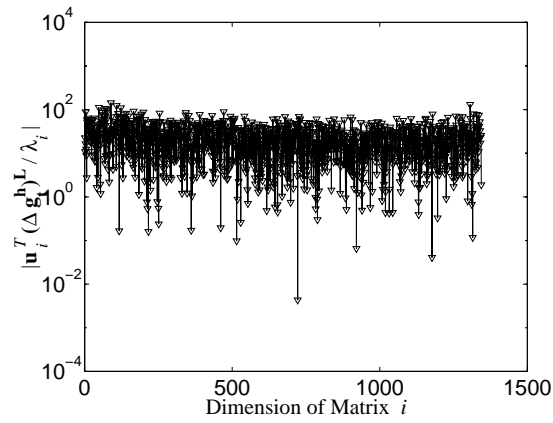
(c) Discrete Picard-Helmert coefficients $\left| \mathbf{u}_i^T \left(\Delta \mathbf{g_t^h} \right)^{\mathbf{L}} \right| / \lambda_i$

Figure 3.10: Discrete Picard plot of $\mathbf{B}_{III}$ in the $2° \times 4°$ block.
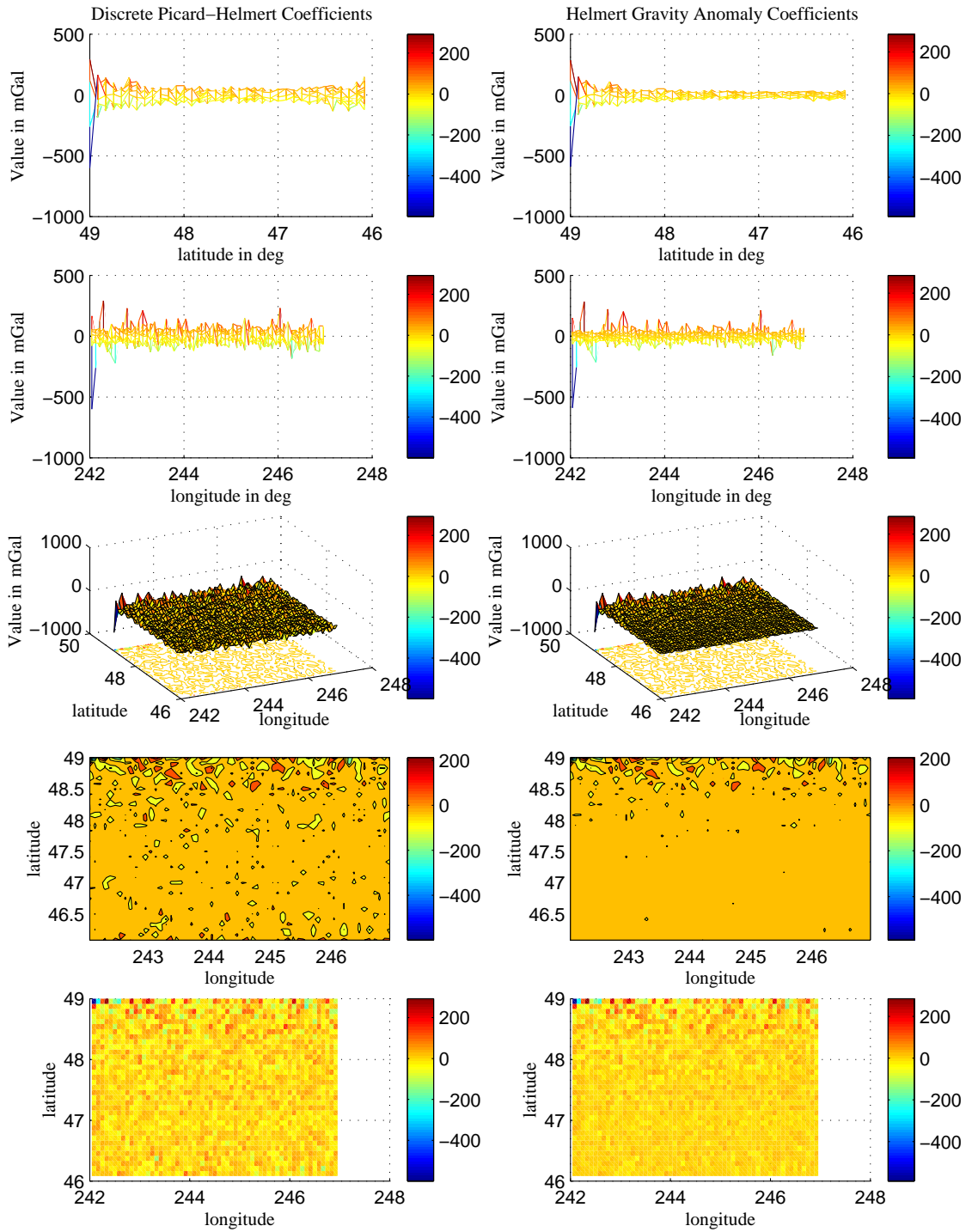
Figure 3.11: A comparison plot of discrete Picard-Helmert coefficients and Helmert gravity anomaly coefficients in the $3° \times 5°$ block of $\mathbf{B}_{III}$ (in mGal).
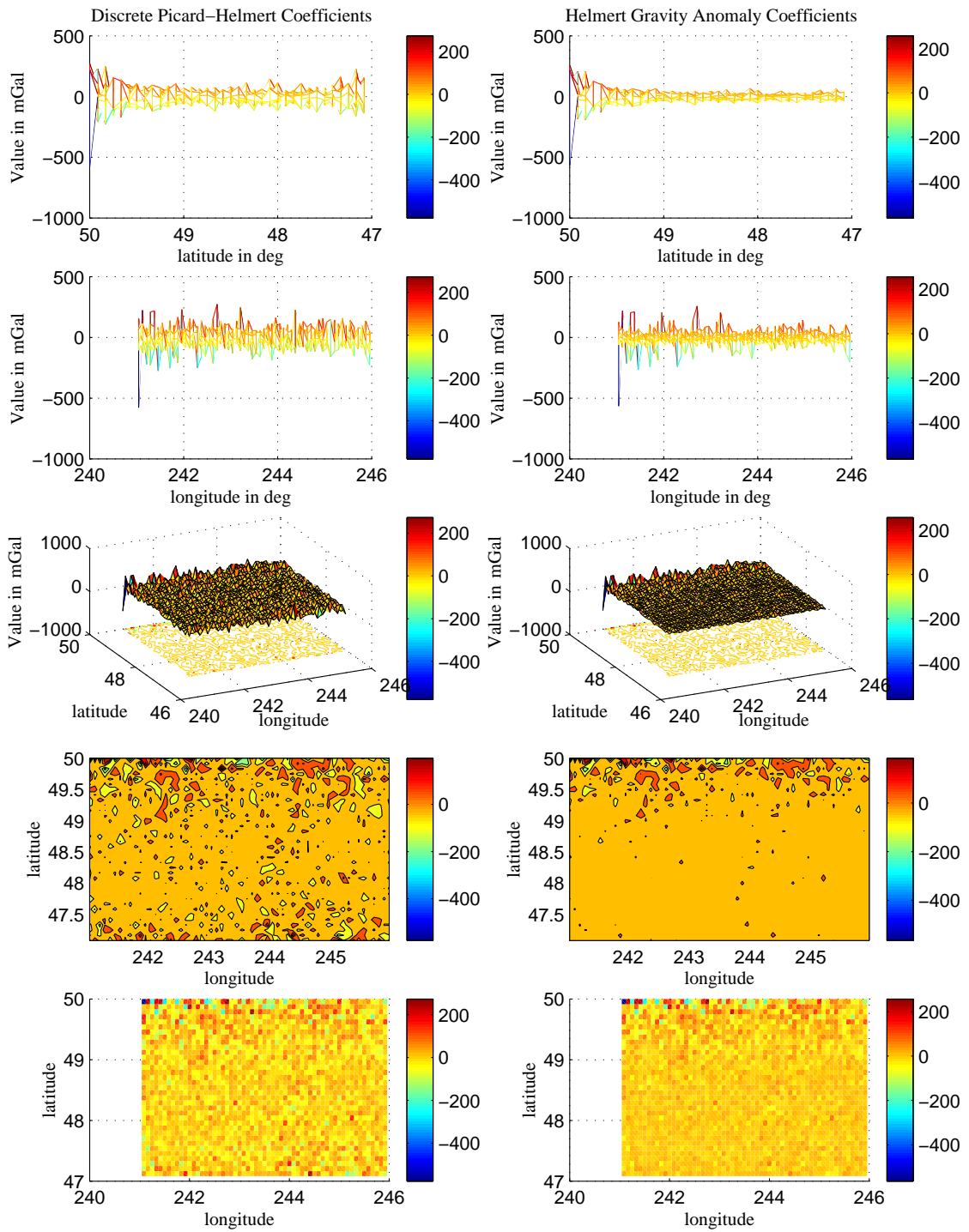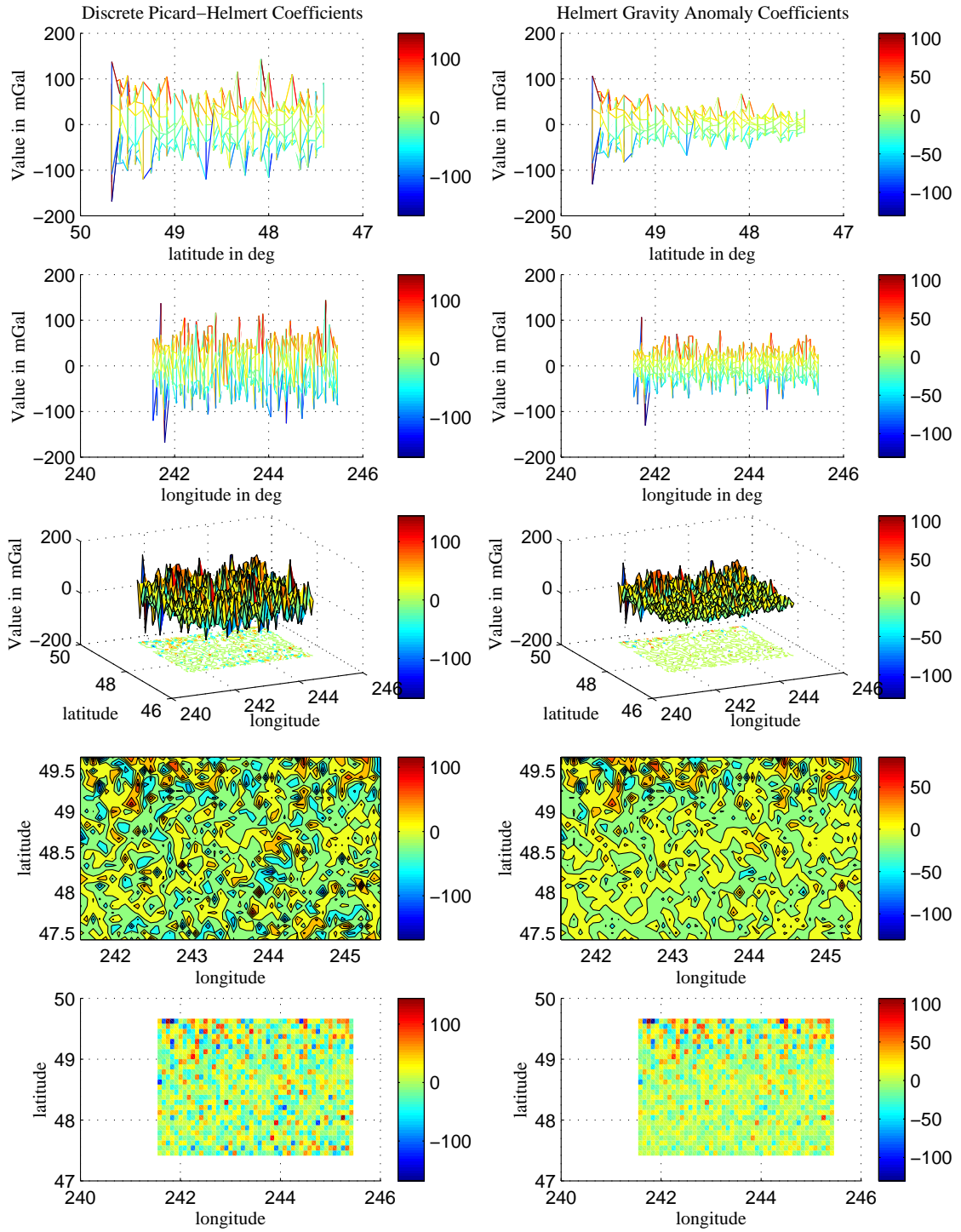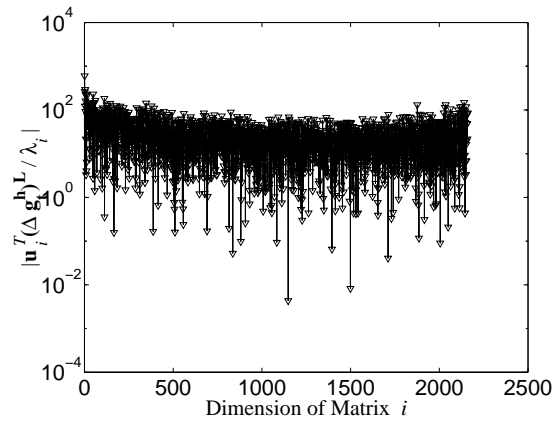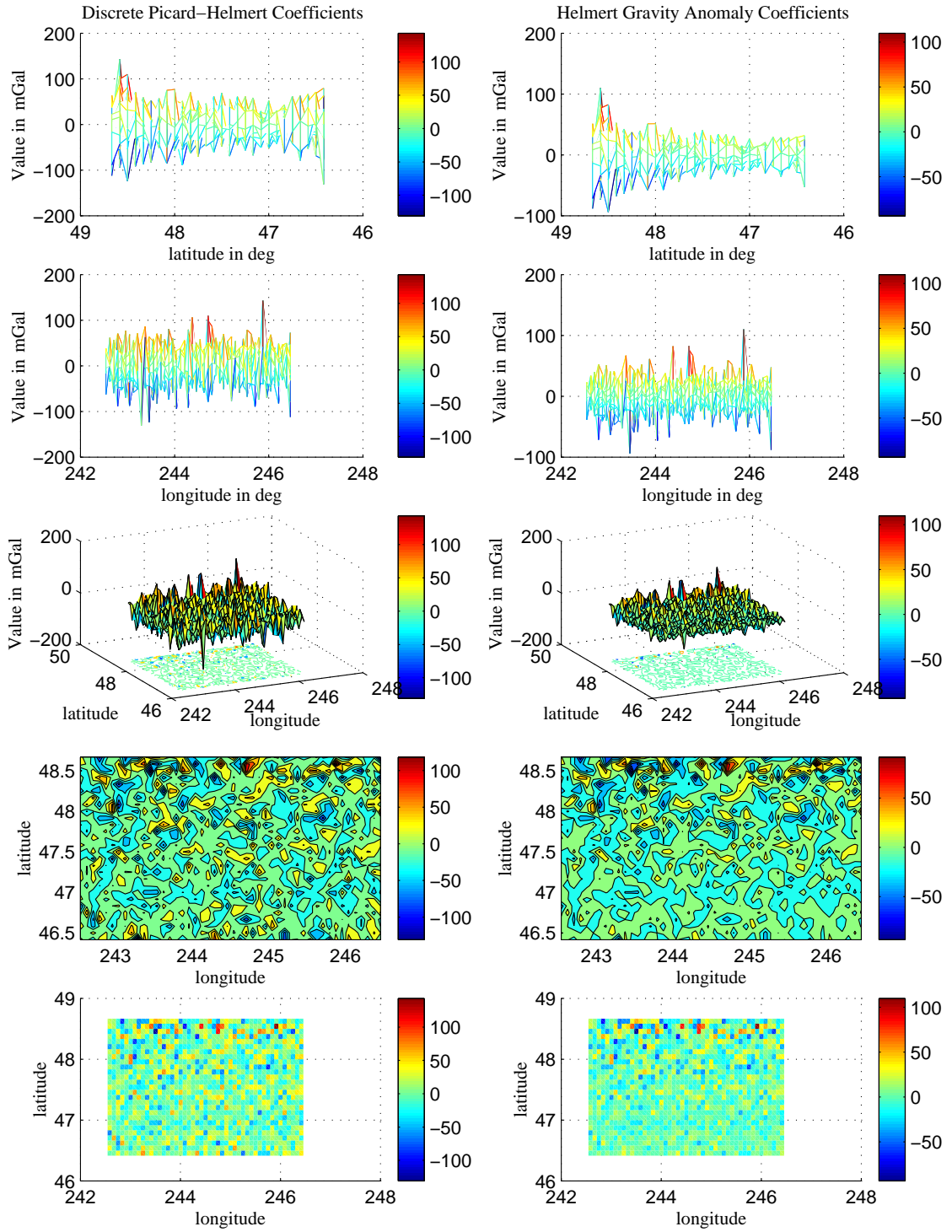
Figure 3.12: A comparison plot of discrete Picard-Helmert coefficients and Helmert gravity anomaly coefficients in the $2° \times 4°$ block of $\mathbf{B}_{III}$ (in mGal).

3.2.2   Analysis of the Boundary Effect

Large oscillations along the boardline of the region of interest are due to the boundary effect. The boundary effect can be caused by

1. the improper numerical computations over the selected area of the spherical cap, and

2. the input data which contains a few blunder data.

Regional Area	Matrix	$\min/\max\{\frac{\mathbf{u}_i^T\left(\Delta\mathbf{g_t^h}\right)^{\mathbf{L}}}{\lambda_i}\}$ mGal	$\min/\max\{\mathbf{u}_i^T\left(\Delta\mathbf{g_t^h}\right)^{\mathbf{L}}\}$ mGal
$49°05'00'' \leq \varphi \leq 52°05'00''$ $239°05'00'' \leq \lambda \leq 244°05'00''$	$\mathbf{B}_I$	-604.7157, 241.4822	-590.6895, 232.5003
$47°05'00'' \leq \varphi \leq 50°05'00''$ $241°05'00'' \leq \lambda \leq 245°55'00''$	$\mathbf{B}_{II}$	-577.7184, 272.8428	-564.5604, 257.4469
$46°05'00'' \leq \varphi \leq 49°05'00''$ $242°05'00'' \leq \lambda \leq 246°55'00''$	$\mathbf{B}_{III}$	-507.7914, 485.4175	-495.0040, 485.3321

Table 3.2: Boundary effect discrepancies between $\frac{\mathbf{u}_i^T\left(\Delta\mathbf{g_t^h}\right)^{\mathbf{L}}}{\lambda_i}$ and $\mathbf{u}_i^T\left(\Delta\mathbf{g_t^h}\right)^{\mathbf{L}}$ in the $3° \times 5°$ area.

(1)   Certain irregular amplitudes located near the edge of the head and tail regions may be seen in Figs. 3.3, 3.7 and 3.11, and due to the incomplete numerical computations over the selected area of the $1°$ cap. In order to iron out the high amplitude of the boundary wiggles along the boarderline, one can reduce the size of the area. For instance, each block can be reduced from $3° \times 5°$ to $2° \times 4°$, as shown in Figs. 3.4, 3.8 and 3.12. Table 3.2 shows the results of the maximum and minimum values of the boundary effect discrepancies between $\frac{\mathbf{u}_i^T\left(\Delta\mathbf{g_t^h}\right)^{\mathbf{L}}}{\lambda_i}$ and $\mathbf{u}_i^T\left(\Delta\mathbf{g_t^h}\right)^{\mathbf{L}}$ in the $3° \times 5°$ area. Table 3.3 shows the results of the maximum and minimum values of the boundary effect discrepancies between $\frac{\mathbf{u}_i^T\left(\Delta\mathbf{g_t^h}\right)^{\mathbf{L}}}{\lambda_i}$ and $\mathbf{u}_i^T\left(\Delta\mathbf{g_t^h}\right)^{\mathbf{L}}$ in the $2° \times 4°$ area.

Regional Area	Matrix	$\min/\max\{\frac{\mathbf{u}_i^T(\Delta\mathbf{g_t^h})^{\mathbf{L}}}{\lambda_i}\}$ mGal	$\min/\max\{\mathbf{u}_i^T(\Delta\mathbf{g_t^h})^{\mathbf{L}}\}$ mGal
$49°35'00'' \leq \varphi \leq 51°35'00''$ $239°35'00'' \leq \lambda \leq 243°35'00''$	$\mathbf{B}_I$	-134.5125, 180.7189	-99.4636, 94.6567
$47°35'00'' \leq \varphi \leq 49°35'00''$ $241°35'00'' \leq \lambda \leq 245°35'00''$	$\mathbf{B}_{II}$	-120.0459, 144.1056	-82.1971, 77.0431
$46°35'00'' \leq \varphi \leq 48°35'00''$ $242°35'00'' \leq \lambda \leq 246°35'00''$	$\mathbf{B}_{III}$	-134.4662, 154.9726	-99.7463,110.6872

Table 3.3: Boundary effect discrepancies between $\frac{\mathbf{u}_i^T(\Delta\mathbf{g_t^h})^{\mathbf{L}}}{\lambda_i}$ and $\mathbf{u}_i^T(\Delta\mathbf{g_t^h})^{\mathbf{L}}$ in the $2° \times 4°$ area.

After reducing the region of interest, the outcomes of the coefficient spectra of Figs. 3.2(a), 3.10(a) and 3.6(a) and 3.2(c), 3.6(c) and 3.10(c) are alike. Using the semi-log graphical representation, as compared with the numerical behaviour of the eigenvalues shown in Figs. 3.1(b), 3.5(b) and 3.9(b) having a nonlinear and exponential shape, Figures. 3.2(b), 3.6(b) and 3.10(b) have a linear profile. This is an indication that, for the spectral profile, the boundary effect could have greatly impacted on the numerical computation of the selected block.

A graphical approach is the most easiest way to make a difference between the finite spectra of the discrete Picard-Helmert and Helmert gravity anomaly coefficients. Throughout these graphical representations, we see how the DPT is used and reflected on these coefficients and the variations from the 2-D to 3-D plots. Figures 3.3, 3.7 and 3.11, and 3.4, 3.8 and 3.12 consist of ten plots. The left- and right-hand sizes of these plots demonstrate the spectra of $\frac{\mathbf{u}_i^T(\Delta\mathbf{g_t^h})^{\mathbf{L}}}{\lambda_i}$ and $\mathbf{u}_i^T(\Delta\mathbf{g_t^h})^{\mathbf{L}}$ with respect to different locations of geographical grid-cells within a specific block, respectively. The first and second rows of these plots illustrate the profile of latitude and longitude against these coefficients. The third rows of these plots are called mesh plots which are drawn as surface graphics objects with the viewpoint of these coefficients along

the z-axis. The fourth rows of these plots are called contour plots which display the isolines of these coefficients, where these coefficients are interpreted as heights with respect to the latitude-longitude plane. The fifth rows of these plots are called filled two-dimensional contour plots (or resolution maps) which display the isolines calculated from these coefficients and fill the areas between the isolines using constant colours.

Figure 3.3 is for the area of $49°05'00'' \leq \varphi \leq 52°05'00''$ N and $239°05'00'' \leq \lambda \leq 243°55'00''$ E with a discrete Picard-Helmert coefficient range of -604.7157 to 241.4822 milligals (mGal). A high coefficient rise is predominate along the boundary coast. Figure 3.4 is for the area of $49°35'00'' \leq \varphi \leq 51°35'00''$ N and $239°35'00'' \leq \lambda \leq 243°35'00''$ E with a discrete Picard-Helmert coefficient range of -134.5125 to 180.7189 milligals (mGal). Pictorially speaking, after shrinking these edges, the finite spectra of the discrete Picard-Helmert and Helmert gravity anomaly coefficients represented by 2-D contour and resolution maps provide us with more stable information.

Figure 3.7 is for the area of $47°05'00'' \leq \varphi \leq 50°05'00''$ N and $241°05'00'' \leq \lambda \leq 245°55'00''$ E with a discrete Picard-Helmert coefficient range of -577.7184 to 272.8428 milligals (mGal). In the mesh plot, a high coefficient drop in the left-hand corner stands out. Figure 3.8 is for the area of $47°35'00'' \leq \varphi \leq 49°35'00''$ N and $241°35'00'' \leq \lambda \leq 245°35'00''$ E with a discrete Picard-Helmert coefficient range of -120.0459 to 144.1056 milligals (mGal). Figure 3.11 is for the area of $46°05'00'' \leq \varphi \leq 49°05'00''$ N and $242°05'00'' \leq \lambda \leq 246°55'00''$ E with a discrete Picard-Helmert coefficient range of -507.7914 to 485.4175 milligals (mGal). In the 2-D (flat shading) contour plot, a mild coefficient drop in the top of the coast line stands out. Figure 3.12 is for the area of $46°35'00'' \leq \varphi \leq 48°35'00''$ N and $242°35'00'' \leq \lambda \leq 246°35'00''$ E with a discrete Picard-Helmert coefficient range of -134.4662 to 154.9726 milligals (mGal). As mentioned earlier, the ususal measure employed in evaluating the variations of these coefficients spectra (namely, the difference between the before and after operation of calculation), proved to be of useful tool in a stability estimate. From

41

Figs. 3.12 and 3.8, we believe that the DPT introduced by this thesis is to provide a complete analysis of the variations of these coefficient spectra, which may put in a new light the analysis of boundary effect.

Blunder Value	min (mGal)	max (mGal)
-3000 mGal	-602.8	510.1
-2000 mGal	-594.2	353.2
-1000 mGal	-585.5	285.1
Normal Value	-577.7	272.8
1000 mGal	-573.1	802.7
2000 mGal	-929.3	1575.7
3000 mGal	-1475.6	2349.4

Table 3.4: A comparison of blunder values of $\mathbf{B}_{II}$.

(2) To demonstrate how the blunder data show high sensitivity to the HDC problem, we add a experimental value into the input data ranging from -3000 mGal to +3000 mGal. For numerical illustration, the following area of coverage of the orthometric height data and Helmert gravity anomalies is used; $47°05'00'' \leq \varphi \leq 50°05'00''$ N, $241°05'00'' \leq \lambda \leq 245°55'00''$ E. The results used with these blunder data are given in Fig 3.13. The maximum and minimum values of discrete Picard-Helmert coefficients for each blunder value are summarized in Table 3.4.

In Fig 3.13, each plot has a remarkably erratic variation and apparent boundary effect along the coastline. It is clearly shown in Figs 3.13 (a) and (f) that a high amplitude, like a ripple, propagates throughout the neighbourhood of the blunder
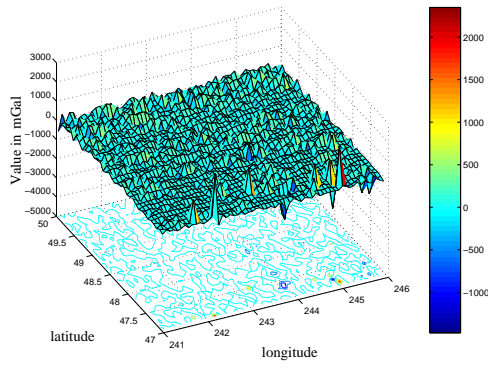
(a) -3000 mGal
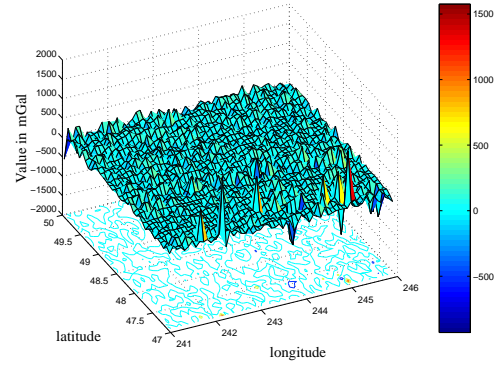
(b) -2000 mGal
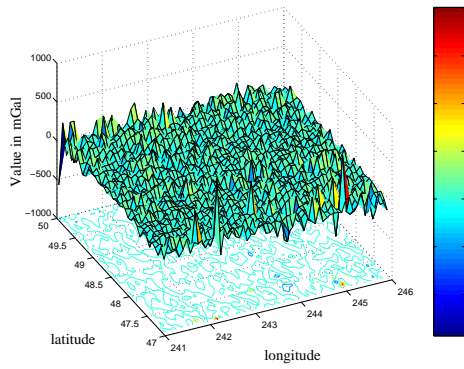
(c) -1000 mGal
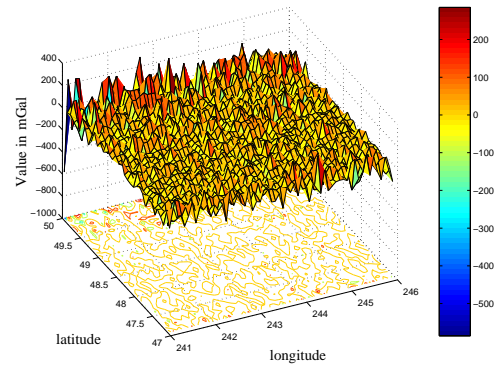
(d) 1000 mGal
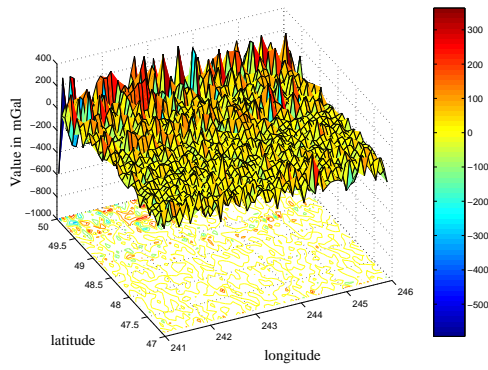
(e) 2000 mGal
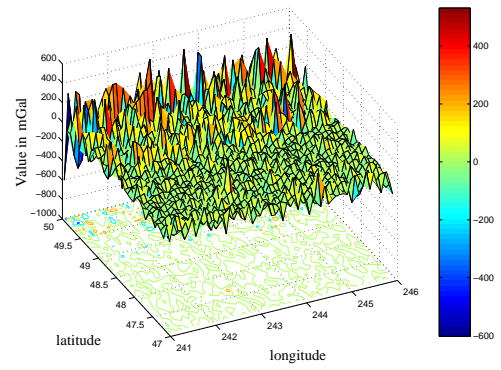
(f) 3000 mGal

Figure 3.13: Plots of blunder data of $\mathbf{B}_{II}$ (in mGal).

value. From the results of Table 3.4, we conclude that outcomes of discrete Picard-Helmert coefficients are significantly magnified by a single blunder value. The blunder value may be occurred by the random errors in measurement. For instance, these pitfalls may be caused by the mis-reading of human's eye-ball. When doing the numerical calculations, one has to detect the blunder data first. If the blunder data is contained in the input values, one simply throws it out.

In this study, one can easily distinguish between the impact of boundary effect and blunder value. It is very often argued that if the physics were properly modelled, the corresponding equations would be well-posed and their solution would not raise difficulties. Under these simplifications, approximations and numerical simulations, the HDC in the NZC leads to the notion of a well-posed problem. However, different sources of errors should not be ignored.

3.2.3 Sources of Errors

The uncertainties of the instability are also caused by different sources of errors. The modelling errors are difficult to quantify and an effective error propagation analysis cannot always be constructed. In these cases the errors in the model are often ignored (Smeets, 1994). Numerical errors are inevitable when doing a numerical computation (Franklin, 1970; Shaw, 1972; Ekstrom and Rhoads, 1974; Hansen, 1998). When using the QEVD, the error $\mathbf{r}_{\mathbf{B}_{\{I,II,III\}}}^{\text{Num.}}$ as the difference between the given solution of $\mathbf{B}$ and computed solution of $\mathbf{B}\mathbf{V}\Lambda^+\mathbf{U}^T$, which consists of the roundoff errors[5] and the truncation errors[6], can be analyzed by the following formula (Kalman, 1996)

$$\mathbf{r}_{\mathbf{B}_{\{I,II,III\}}}^{\text{Num}} = \left(\Delta\mathbf{g_t^h}\right)^{\mathbf{L}} - \mathbf{B}\mathbf{V}\Lambda^+\mathbf{U}^T\left(\Delta\mathbf{g_t^h}\right)^{\mathbf{L}}, \tag{3.2.8}$$

---

[5]Roundoff error arises from the fact that computer arithmetic is not exact (i.e., Pizer and Wallace, 1983).

[6]Truncation error arises from the use of approximate formulæ that are not exact "even in exact arithmetic" (i.e., Pizer and Wallace, 1983).

and the computed magnitude of the numerical errors ϵ^{Num} is given by

$$\epsilon^{\mathrm{Num}} = \left(\mathbf{r}^{\mathrm{Num}}_{\mathbf{B}_{\{I,II,III\}}}{}^{T} \cdot \mathbf{r}^{\mathrm{Num}}_{\mathbf{B}_{\{I,II,III\}}} \right)^{1/2} . \qquad (3.2.9)$$

Based on the IEEE floating-point arithmetic in a double precision, where $eps = 2.22e - 16$, MATLAB responds with $\epsilon^{\mathrm{Num}} \approx 10^{-14}$ which is close to the order of magnitude of the eps. From the numerical results, we see that the numerical errors can be ignored. Contaminated errors on the data seem to be significantly larger than the modelling and numerical errors and vary from one observation to another. The best choice for analyzing the error propagation of the HDC problem is stochastic modelling. Its development is still in infancy, which leads to the other unanswered question on how the HDC is affected by the random errors. And the another unanswered question will provide an answer whether the random errors of the HDC is a well-posed problem or not (Vaníček and Wong, 2000).

Chapter 4

Conclusion and Further Research

4.1 Conclusion

The QEVD provided well-posed results in Chapter 4 in the sense of Hadamard by mean of the DPT. The well-posed nature of the HDC problem in the NZC seems to manifest itself in the finite discretization $5' \times 5'$ step of the mean Helmert gravity anomaly within the radius of spherical cap $\psi_0 = 1°$ leading to the generation of a well-conditioned square matrix by means of the magnitude of the condition number.

From a numerical viewpoint, several computations have shown that the smallest digit of the final solutions may not be necessary to reach the maximum threshold of the floating point relative accuracy. With our present technology, it is hard to characterize the actual behaviour of the final outcomes in a microscopic investigation because of the limit of time consumptions and sufficient accuracies. As long as the size of computational storage does not go beyond the relative accuracy for each computers capacity, the HDC in the NZC is a well-posed problem.

4.2   Further Research

Feasible areas for further work that are related to this thesis are:

1. One can show the sum of the two ellipsoidal corrections is a harmonic function of 3-D position.

2. The truncation error on the Helmert co-geoid can be formulated as an inverse probelm.

3. Using the discrete Picard technique, one can examine the existence and stability of a solution of the truncation error, referred to as the spectral analysis of the HDC problem in the FZC.

4. Because the above conclusions are based on a discrete model, one can use them as a starting point for determining some margins of error propagation from the measurements and the numerical integration schemes in a worst scenario situation.

5. One difficulty in determining the Helmert gravity anomalies on the Helmert co-geoid in general is that they tend to need a great deal of computational time for a large area of interest: typically they involve solving the inverse matrix of non-symmetric cases, which can be done using either a direct method or an iterative method. Recently, the invention of the so-called Conjugate Gradient method, which is an iterative method that increases the rate of convergence and the speed of computation by means of the non-stationary (or non-symmetric) iterative methods, has resulted in the development of the following items: including BiCongugate Gradients, BiConjugate Gradients Stabilized, Generalized Minimum Residual, Quasi-Minimal Residual and other methods. For a detailed information, see Barrett *et al.* (1994) and Demmel (1997).

Bibliography

Allen, R. C., Jr., W. R. Boland and G. M. Wing. (1983). Numerical experiments involving Galerkin and collocation methods for linear integral equations of the first kind. *Journal of Computational Physics*, **49**, pp. 465-477.

Anderson, E. G., C. Rizos and R. S. Mather. (1975). Amtospheric effects in physical geodesy. UNISURV G 23, pp. 23-41, University of New South Wales, Sydney, Australia.

Archibald, T. (1989). Connectivity, and Smoke-Rings: Green's Second Idenity in Its First Fifty Years. *Mathematics Magazine*, Vol. **62**, No.4, pp. 219-232.

Balmino, G. (1983). A few remarks on the Earth's atmosphere effects on the geoid, the free-air anomalies, the altimetric geoid, and combination procedures in global geopotential model computation. *Bulettin d'Information*, **53**, Bureau Gravimetrique International, Brussels.

Barrett, R., M. W. Berry, T. F. Chan, J. Demmel, J. Donato, J. Dongarra, V. Eijkhout, R. Pozo, C. Romine, and H. van der Vorst. (1994). *Templates for the Solution of Linear Systems: Building Blocks for Iterative Methods*. SIAM, Philadelphia.

Bateman, H. (1908). A formula for the solving function of a certain integral equation of the second kind. *Transactions of the Cambridge Philosophical Society*, **20**, pp. 179-187.

Bitsadze, A. V. (1995). *Integral Equations of First Kind.* Series on Soviet & East European Mathematics - Vol. 7, World Scientific, Singapore, New Jersey, London, Hong Kong.

Bjerhammar, A. (1962). Gravity reduction to a spherical surface. The Royal Institute of Technology, Stockholm.

Bjerhammar, A. (1964). A new theory of gravimetric geodesy. Rep. **243**, Transaction Royal Institute of Technology, Stockholm.

Bjerhammar, A. (1973a). On the discrete boundary value problem in physical geodesy. The Royal Institute of Technology, Division of Geodesy, Stockholm.

Bjerhammar, A. (1973b). *Theory of Errors and Generalized Matrix Inverses.* Elsevier, Amsterdam.

Bjerhammar, A. (1975). Discrete solutions of the boundary value problem in physical geodesy. *Tellus*, **II**, pp. 97-105.

Bjerhammar, A. (1976). A Dirac approach to physical geodesy. *Zeitschrift für Vermessungswesen*, **2**, pp. 41-44.

Bjerhammar, A. (1987). Discrete physical geodesy. Rep. **380**, Department of Geodetic Science and Surveying, The Ohio State University, Columbus, USA.

Björck, A. (1996). *Numerical Methods for Least Squares Problems.* SIAM, Philadelphia.

Bleecker, D. and G. Csordas. (1992). *Basic Partial Differential Equations.* Van Nostrand reinhold, New York.

Bomford, G. (1962). *Geodesy* (2nd edn). Oxford University Press.

Branham, Jr., R. (1980). Least-squares solution of ill-conditioned systems. *The Astronomical Journal*, **84**, pp. 1632-1637.

Branham, Jr., R. (1980). Least-squares solution of ill-conditioned systems. II. *The Astronomical Journal*, **85**, pp. 1520-1527.

Bullard, E. C. (1936). Gravity measurements in East Africa. *Transactions of the Royal Society of London*, **235**, pp. 486-497.

Caputo, M. (1967). *The Gravity Field of the Earth - from Classical and Modern Methods*. Academic Press, New York, London.

Churchill, R. V. and J. W. Brown. (1987). *Fourier Series and Boundary Value Problems*. 4th ed., McGraw-Hill, New York.

Colombo, O. L. (1981). Numerical methods for harmonic analysis on the sphere. Rep. **310**, Department of Geodetic Science and Surveying, The Ohio State University, Columbus, USA.

Cruz, J.Y. (1985). Disturbance vector in space from surface gravity anomalies using complementary models. Rep. **366**, Department of Geodetic Science and Surveying, The Ohio State University, Columbus, USA.

Cruz, J.Y. (1986). Ellipsoidal corrections to potential coefficients obtained from gravity anomaly data on the ellipsoid. Rep. **371**, Department of Geodetic Science and Surveying, The Ohio State University, Columbus, USA.

Dancer, N. (1998). Private Communication.

Davis, P. (1963). *Interpolation & Approximation*. Dover Publications, New York.

Demmel, J. W. (1997). *Applied Numerical Linear Algebra*. SIAM Press, Philadelphia.

de Witte, L. (1967). Truncation errors in the Stokes and Vening Meinesz formulæ for differenting order spherical harmonic gravity. *The Geophysical journal of the Royal Astronomical Society*, **12**, pp. 449-464.

Diviš, K., J. Trešl and J. Kostelecý. (1981). Effect of the anomalous part of the atmosphere on the observed acceleration of gravity. *Studia geophysica & geodætica*, **25**, pp. 321-331.

Dongarra, J.J., J.R. Bunch, C.B. Moler, and G.W. Stewart. (1979). *LINPACK Users' Guide*. SIAM, Philadelphia. http://www.netlib.org/lapack/

Ecker, E. (1968). The effect of the atmosphere on the theory of the level ellipsoid. *Bollettino di Geofisica Teorica ed Applicata*, **X(38)**, pp. 70-80.

Ecker, E. (1970). Über die räumliche Konvergenz von Kugelfunktionsreihen. Deutsche Geodätische Kommission, Reihe C, Heft Nr. 68, München.

Ecker, E. and E. Mittermayer. (1969). Gravity Corrections for the influence of the Atmosphere. *Bollettino di Geofisica Teorica ed Applicata*, **II(41)**, pp. 70-80.

Eldén, L. (1993). The numerical solution of a non-characterictic Cauchy problem for a parabolic equation. In: *Numerical Treatment of Inverse Problems in Differential and Integral Equations*, eds. P. Deuflhard, E. Hairer, Birkhäuser, Boston, Basel, Stuttgart.

Engels, J., E. Grafarend, W. Keller, Z. Martinec, F. Sansò, P. Vaníček. (1993). The Geoid as Inverse Problem to be Regularized. In: *Inverse Problems: Principles and Applications in Geophysics, Technology, and Medicine*, eds. G. Anger, R. Gorenflo, H. Jochmann, H. Mortiz, W. Webers, Akademie Verlag GmbH, Berlin.

Engl, H. W. (1982). On Least-Squares Collocation for Solving Linear Integral Equations of the First Kind with Noisy Right-Hand Side. *Bollettino di Geodesia e Scienze Affini*, **41**, pp. 291-313.

Ekstrom, M. and R. Rhoads. (1974). On the application of eigenvector expansions to numerical deconvolution. *Journal of Computational Physics*, **14**, pp. 319-340.

Featherstone, W. E., J.D. Evans and J. G. Olliver. (1998). A Meissl-modified Vaníček and Kleusberg kernel to reduce the truncation error in gravimetric geoid computations. *Journal of Geodesy*, **72**, pp. 154-160.

Forsberg, R. and C. C. Tscherning. (1997). Topographic effects in gravity field modelling for BVP. In: *Geodetic Boundary Value Problems in View of the One Centimeter Geoid*, eds. F. Sansò and R. Rummel, Lecture Notes in Earth's Sciences, **65**, Springer-Verlag, Berlin, Heidelberg, New York.

Franklin, J. N. (1970). Well-posed stochastic extensions of ill-posed linear problems. *Journal of Mathematical Analysis and Applications*, **31**, pp. 682-716.

Fredholm, E. I. (1900). Sur une nouvelle méthode pour la résolution du problème de Dirichlet. Öfversigt af Kongliga Svenska Vetenskaps-Akademiens Förhandlingar Stockholm, t. **131**, pp. 39-46.

Gauß, C. F. (1886). Theoria interpolationis methodo nova tractata. Gauß's Collected Works Volume 3, pp. 265-303.

Gerstl, M. and R. Rummel. (1981). Stability investigations of various representations of the gravity field. *Reviews of Geophysics and Space Physics*, **19**, pp. 415-420.

Golub, G. and C. Van Loan. (1983). *Matrix Computations*. Johns Hopkins University Press, MD.

Grafarend, E. K. (1972). Inverse potential problems of improperly posed type in physical geodesy and geophysics. Contribution Presented to the International Symposium on Earth Gravity Models and Related Problems, Saint Louis, Missouri, August 16-18.

Grafarend, E. K. (1975). Geodetic applications of stochastic processes. Contribution Presented to the IVGG - Generaly Assembly, Grenoble, France.

Groetsch, C. W. (1984). *The Theory of Tikhonov Regularization for Fredholm Equation of the First Kind.* Pitman, London.

Groetsch, C. W. (1993). *Inverse Problems in the Mathematical Sciences.* Braunschweig; Wiesbaden: Vieweg.

Gronwall, T. H. (1913). On the degree of convergence of Laplace's series. *Transactions of the American Mathematical Society*, **1**, pp. 1-30.

Gustafson, K. (1987). *Introduction to Partial Differential Equations and Hilbert Space Methods.* Wiley, 2nd Edition, New York.

Gustafson, K. and T. Abe. (1998a). The third boundary condition - was it Robin's?. *The Mathematical Intelligencer*, **20**, No. 1, pp. 63-71.

Gustafson, K. and T. Abe. (1998b). (Victor) Gustave Robin: 1855-1897. *The Mathematical Intelligencer*, **20**, No. 2, pp. 47-53.

Hadamard, J. (1902). Sur les problèmes aux dérivées partielles et leur signification physique. *Princeton University Bulletin*, **13**, pp. 1-20.

Hadamard, J. (1923). *Lectures on the Cauchy Problem in Linear Partial Differential Equations..* Yale University Press, New Haven.

Hanke, M. and P. C. Hansen. (1993). Regularization methods for large-scale problems. *Surveys On Mathematics for Industry*, **3**, pp. 253-315.

Hansen, P. C. (1988). Computation of the singular value expansion, *Computing*, **40**, pp. 185-199.

Hansen, P. C. (1990). The discrete Picard technique for discrete ill-posed problems. *BIT*, **30**, pp. 658-672.

Hansen, P. C. (1998). *Rank-Deficient and Discrete Ill-Posed Problems.* SIAM, Philadelphia.

Hanson, R. J. (1971). A numerical method for solving Fredholm integral equations of the first kind using singular values. *SIAM Journal on Numerical Analysis*, **8**, pp. 616-622.

Heck, B. (1991a). A revision of Helmert's second method of condensation in geoid and quasigeoid determination. In: *Geodesy and Physics of the Earth*, ed. H. Montag and C. Reigber, International Assiocation of Geodesy Sympoisa, Vol. 112, Springer Verlag, Berlin, Heidelberg, New York, pp. 246-251.

Heck, B. (1991b). On the linearized boundary value problems of physical geodesy. Rep. **407**, Department of Geodetic Science and Surveying, The Ohio State University, Columbus, USA.

Heck, B. and W. Grüninger. (1987). Modification of Stokes's integral formula by combining two classical approaches. The International Union of Geodesy and Geophysics (IUGG) General Assembly, Vancouver.

Heiskanen, W. A. and H. Moritz. (1967). *Physical Geodesy*. W.H. Freeman and Co., San Francisco, Londres.

Helmert, F. R. (1884). *Die Mathematischen und Physikalischen Theorieen der Höheren Geodäsie, II. Teil.* Teubner, Leipzig. Reprint Minerva GMBH, Frankfurt/Main 1962.

Herr, D. G. (1974). On a statistical model of Strand and Westwater for the numerical solution of a Fredholm integral equation of the first kind. *Journal of the Association for Computing Machinery*, **21**, pp. 1-5.

Hofmann-Wellenhof, B., and H. Moritz. (1986). Introduction to spectral analysis. In: Mathematical and Numerical Techniques in Physical Geodesy, ed. H. Sünkel, Lecture Notes in Earth Sciences, No. 7, Springer-Verlag, Berlin, Heidelberg, New York, London, Paris, Tokyo.

Holota, P. (1987). Boundary value and convergence problems in physical geodesy. In: *Contributions to Geodetic Theory and Methodology*, XIX General Assembly of the IUGG, IAG, Section IV, Vancouver, B.C., Canada, August 9-22, pp. 73-96.

Hömander, L. (1975). The boundary problems of physical geodesy. The Royal Institute of Technology, Division of Geodesy, Stockholm; also in: *Archive for Rational Mechanics and Analysis*, **62**(1976), pp. 1-52.

Hotine, M. (1969). *Mathematical Geodesy*, ESSA Monography 2, U.S. Department of Commerce.

Ilk, K. H. (1987). On the regularization of ill-posed problems. In: *Figure and Dynamics of the Earth, Moon, and Planets*, ed. P. Holota, Research Inst. of Geodesy, Topography and Cartography, Prague, pp. 365-383.

Ilk, K. H. (1993). Regularization for high resolution gravity field recovery by future satellite techniques. In: *Inverse Problems: Principles and Applications in Geophysics, Technology, and Medicine*, eds. G. Anger, R. Gorenflo., H. Jochmann, H. Moritz and W. Webers, pp. 189-214.

Jekeli, C. (1981a). The downward continuation to the Earth's surface of truncated spherical and ellipsoidal harmonic series of the gravity and height anomalies. Rep. **323**, Department of Geodetic Science and Surveying, The Ohio State University, Columbus, USA.

Jekeli, C. (1981b). Modifying Stokes's function to reduce the error of geoid undulation computations. *Journal of geophysical research*, **86**(B8), pp. 6985-6990.

Kalman, D. (1996). A singularly valuable decomposition: the SVD of a matrix. *The College Mathematics Journal*, **27**, pp. 2-23.

Karl, J. H. (1971). The Bouguer correction for the spherical earth. *Geophysics*, **36**, pp. 761-762.

Kaula, W. M. (1966). *Theory of satellite Geodesy*, Blaisdell, Waltham, Mass.

Kellogg, O. D. (1926). Recent progress with the Dirichlet problem. *American Mathematical Society*, **32**, pp. 601-625.

Kellogg, O. D. (1967). *Foundations of Potential Theory*. Springer, Berlin, Heidelberg, New York (reprinted by Dover Publications, New York, 1953).

Kleusberg, A. and P. Vaníček. (1991). Gravity correction in Helmert's condensation. Unpublished manuscripts.

Krarup, T. (1969). A Contribution to the Mathematical Foundation of Physical Geodesy. Rep. **44**, Geodætisk Institu, København.

LaFehr, T. R. and K. C. Chan. (1986). Discussion on "The normal vertical gradient of gravity: by J. H. Karl, (*Geophysics*, **48**, pp. 1011-1013, July 1983): *Geophysics*, **51**, pp. 1505-1508.

LaFehr, T. R. (1991a). Standardization in gravity reduction. *Geophysics*, **56**, pp. 1170-1178.

LaFehr, T. R. (1991b). An exact solution for the gravity curvature (Bullard B). *Geophysics*, **56**, pp. 1179-1184.

Lambert, W. D. (1930). The reduction of observed values of gravity to sea level. *Bulletin Géodésique*, **53**, pp. 343-361.

Landweber, L. (1951). An iteration formula for Fredholm integral equations of the first kind. *American Mathematical Society*, **26**, pp. 107-181.

Lavrentiev, M. M. (1967). *Some Improperly Posed Problems of Mathematical Physics*. Translation revised by Robert J. Sacker. Springer-Verlag, New York Inc..

Lemoine, F. G., *et al.* (1996). The development of the NASA GSFC and DMA joint geopotential model. Proceedings of International Symposium on Gravity, Geoid and Marine Geodesy. Tokyo, Japan, Sept 30 - Oct 5, pp. 461-469.

Lerch, F. J., *et al.* (1994). A geopotential model for the Earth from satellite tracking, altimeter, and surface gravity observations: GEM-T3. *Journal of Geophysical Research*, **99**, pp. 2815-2839.

Levenberg, K. (1944). A method for the solution of certain nonlinear problems in least-squares. *Quarterly of Applied Mathematics*, **2**, pp. 164-166.

Li, Y. C. (1993). Optimized spectral geoid determination. UCSE Report #20050, Division of Surveying Engineering, University of Calgary, Calgary, Alberta, Canada.

Listing, J. B. (1873). Ueber unsere jetzige Kenntniss der Gestalt und Grösse der Erde. *Königliche Gesellschaft der Wissenschaften*, pp. 33-98.

Love, A. E. H. (1911). *Some Problems of Geodynamics.* Reprinted by Dover Publications, New York, 1967.

Lukeš, J. and I. Netuka. (1979). What is the right solution of the Dirichlet problem? Romanian-Finnish Seminar on Complex Analysis (Proc., Bucharest, 1976), pp. 564 - 572. Lecture Notes in Mathematics, **743**, Springer Verlag, Berlin, Heidelberg, New York.

MacMillan, W. D. (1958). *The Theory of the Potential.* Dover Publications, New York.

Madden, S. J., Jr. (1972). A simplified model for the gravitational potential of the atmosphere and its effect on the geoid. Rep. **84**, Massachusetts Institute of Technology.

57

Marsh, J., F. Lerch, B. Putney, T. Felsentregger, B. Sanchez, S. Klosko, G. Patel, J. Robbins, R. Williamson, T. Engelis, W. Eddy, N. Chandler, D. Chinn, S. Kapoor, K. Rachlin, L. Braatz and E. Pavlis. (1990). The GEM-T2 gravitational model. *Journal of Geophysical Research*, **95**, (B13), pp. 22043-22071.

Martinec, Z., C. Matyska, E. W. Grafarend, and P. Vaníček. (1993). On Helmert's 2$^{\text{nd}}$ condensation method. *Manuscripta geodætica*, **18**, pp. 417-421.

Martinec, Z. and P. Vaníček. (1994a). The indirect effect of topography in the Stokes-Helmert technique for a spherical approximation of the geoid. *Manuscripta geodætica*, **19**, pp. 213-219.

Martinec, Z. and P. Vaníček. (1994b). Direct topographical effect of Helmert's condensation for a spherical approximation of the geoid. *Manuscripta geodætica*, **19**, pp. 257-268.

Martinec, Z. (1996). Stability investigations of a discrete downward continuation problem for geoid determination in Canadian Rocky Mountains. *Journal of Geodesy*, **70**, pp. 805-828.

Martinec, Z. (1998). Boundary-Value Problems for Gravimetric Determination of a Precise Geoid. Lecture Notes in Earth Sciences, **73**, Springer Verlag, Berlin, Heidelberg, New York.

MATLAB, student ed. (1999). Prentice Hall, Englewood Cliffs, NJ.

McCarthy, D. (1996). IERS Conventions (1996). IERS TECHNICAL NOTE 21, U.S. Naval Observatory.

Meissel, P. (1971a). Preparations for the numerical evaluation of second-order Molodensky-type formulas. Rep. **163**, Department of Geodetic Science and Surveying, The Ohio State University, Columbus, USA.

Meissel, P. (1971b). On the linearisation of the geodetic boundary value problem. Rep. **152**, Department of Geodetic Science and Surveying, The Ohio State University, Columbus, USA.

Molodenskij, M. S., V. F. Eremeev and M. I. Yurkina. (1962). *Methods for study of the external gravitational field and figure of the Earth.* Translated from the Russian (1960) by the Israel Program for Scientific Translations, Jerusalem, for Office of Technical Services, Department of Commerce, Washington, DC.

Moritz, H. (1966a). Linear Solutions of the Geodetic Boundary-Value Problem. Rep. **79**, Department of Geodetic Science and Surveying, The Ohio State University, Columbus, USA.

Moritz, H. (1966b). Methods for Downward Continuation of Gravity. Deutsche Geodätische Kommission, Reihe C, Heft Nr. 50, München.

Moritz, H. (1968). On the Use of the Terrain Correction in Solving Molodensky's Problem. Rep. **108**, Department of Geodetic Science and Surveying, The Ohio State University, Columbus, USA.

Mortiz, H. (1971). Series Solutions of Molodensky's Problem. Deutsche Geodätische Kommission, Reihe C, Heft Nr. 70, München.

Mortiz, H. (1974). Precise Gravimetric Geodesy. Rep. **219**, Department of Geodetic Science and Surveying, The Ohio State University, Columbus.

Moritz, H. (1980). *Advanced Physical Geodesy.* Herbert Wichmann Verlag, Karlsruhe.

Mortiz, H. (1990). *The figure of the Earth: theoretical geodesy and the Earth's interior.* Herbert Wichmann Verlag, Karlsruhe.

Moritz, H. (1992). Geodetic Reference System 1980. In: *The Geodesist's Handbook*, Ed. C. C. Tschering, IAG, Paris.

Mulcahy, C. and J. Rossi. (1998). A fresh approach to the singular value decomposition. *The College Mathematics Journal*, **29**, pp. 199-207.

Needham, T. (1994). The Geometry of Harmonic Functions. *Mathematics Magazine*, **67**, pp. 92-108.

Needham, T. (1997). *Visual Complex Analysis*. Clarendon Press, Oxford.

Nerem, R. S., *et al.* (1994). Gravity model development for TOPEX/POSEIDON: Joint Gravity Model 1 and 2. *Journal of Geophysical Research*, **99(C12)**, pp. 24421-24447.

Neumann, C. (1877). *Untersuchungen über das logarithmische und Newtinsche Potential.* Teubner Verlag, Leipzig.

Neyman, Y. M. (1985). Improperly posed problems in geodesy and methods of their solution. In: Proceedings of the International Summer School on Local Field Approximation, Beijing, UCSE Report #60003, Division of Surveying Engineering, University of Calgary, Calgary, Alberta, Canada.

Novák, P. (1999). *Evaluation of gravity data for the Stokes-Helmert solution to the geodetic boundary-value problem.* Ph.D. thesis in Geodesy and Geomatics Engineering, University of New Brunswick.

Paul, M. K. (1973). A method of evaluating the truncation error coefficients for geoidal height. *Bulletin Géodésique*, **47**, pp. 413-425.

Payne, L. E. (1975). *Improperly Posed Problems in Partial Differential Equations.* SIAM Publications, Philadelphia.

Pavlis, E. (1998). ftp://geodesy.gsfc.nasa.gov/dist/EGM96/

Petrovskaya, M. S. and K. V. Pischukhina. (1990) Methods for compact approximation of geoid height. *Manscripta Geodætica*, **15**, pp. 253-260.

Phillips, D. L. (1962). A technique for numerical solution of certain integral equations of the first kind. *Journal of the Association for Computing Machinery*, **9**, pp. 84-97.

Picard, E. (1910). Sur un théorème général relatif aux équations intégrales de première espèce et sur quelques problèms de physique mathématique. *Rendicondi der Circolo Matematico di Palermo*, **29**, pp. 79-97.

Pick, M., J. Pícha and V. Vyskočil. (1973). *Theory of the Earth's Gravity Field.* Elsevier Scientific Publishing Company, Amsterdam, London, New York.

Pizer, S. M. and V. L. Wallace. (1983). *To Compute Numerically: Concepts and Strategies.* Little, Brown and Company, Boston, Toronto.

Rapp, R. H. and R. Rummel. (1975). Methods for the computation of detailed geoids and their accuracy. Rep. **233**, Department of Geodetic Science and Surveying, The Ohio State University, Columbus.

Rapp, R. H., and J. Y. Cruz. (1986). Spherical harmonic expansions of the Earth's gravitational potential to degree 360 using $30'$ mean anomalies. Rep. **376**, Department of Geodetic Science and Surveying, The Ohio State University, Columbus, USA.

Rapp, R. H., Y. M. Wang and N. K. Pavlis. (1991). The Ohio State 1991 geopotential and sea surface topography harmonic coefficient models. Rep. **410**, Department of Geodetic Science and Surveying, The Ohio State University, Columbus.

Rapp, R. H. (1997). Past and future developments in geopotential modelling. In: *Geodesy on the Move - Gravity, Geoid, Geodynamics and Antarctica*, eds. R.

Forsberg, M. Feissel and R. Dietrich, International Association of Geodesy Symposia, Vol. **119**, Springer-Verlag, Berlin, Heidelberg, New York.

Ren, H. (1996). *On the error analysis and implementation of some eigenvalue decomposition and singular value decomposition algorithms.* Ph.D. thesis in Applied Mathematics, University of California at Berkeley.

Rummel, R. and R. Rapp. (1976). The influence of the atmosphere on geoid and potential coefficient determinations from gravity data. *Journal of geophysical research*, **81**, pp. 5639-5642.

Rummel, R., K. P. Schwartz. and M. Gerstl. (1979). Least squares collocation and regularization. *Bulletin Géodésique*, **53**, pp. 343-361.

Rummel, R. (1997). Spherical spectral properties of the Earth's gravitational potential and its first and second derivatives. In: *Geodetic Boundary Value Problems in View of the One Centimeter Geoid*, eds. F. Sansò and R. Rummel, Lecture Notes in Earth's Sciences, Vol. **65**, Springer-Verlag, Berlin, Heidelberg, New York.

Runge, C. (1884). Zur theorie der eindeutigen analytischen functionen. *Acta Mathematica*, **6**, pp. 229-224.

Sansò, F. (1977). The geodetic boundary value problem in gravity space. Atti Acc. Naz. Lencei, Cl. Sc. Fis. Mat. Nat., Memorie, S. VII, vol. XIV, pp, 41-97.

Sansò, F. (1997). The Hierarchy of Geodetic BVPs. In: *Geodetic Boundary Value Problems in View of the One Centimeter Geoid*, eds. F. Sansò and R. Rummel, Lecture Notes in Earth's Sciences, **65**, Springer-Verlag, Berlin, Heidelberg, New York.

Schaffrin, B., E. D. Heidenreich and E. Grafarend. (1977). A representation of the standard gravity field. *Manscripta Geodætica*, **2**, pp. 135-174.

Schmidt, E. (1907). Zur theorie der linearen und nichtlinearen integralgleichungen. *Mathematische Annalen*, **63**, pp. 433-476.

Schwartz, K. P. (1971). Numerische Untersuchungen zur Schwerefortsetzung. Deutsche Geodätische Kommission, Reihe C, Heft Nr. 171, München.

Schwartz, K. P. (1978). Geodetic improperly posed problems and their regularization. Lecture Notes of the Second International School of Advanced Geodesy, Erice.

Schwartz, K. P. (1984). Data types and their properties. In: Proceedings of the International Summer School on Local Gravity Approximation, Beijing, UCSE Report #60003, Division of Surveying Engineering, University of Calgary, Calgary, Alberta, Canada.

Schwartz, K. P., M. G. Siders and R. Forsberg. (1990). The use of FFT techniques in physical geodesy. *Geophysical Journal International*, **100**, pp. 485-514.

Schwintzer P., *et al.* (1997). Long-wavelength global gravity field models: GRIM4-S4, GRIM-C4. *Journal of Geodesy*, **71**, pp. 189-208.

Seeber, G. (1993). *Satellite Geodesy: Foundations, Methods, and Applications*. Walter de Gruyter & Co., Berlin, New York.

Shaw, C. B., Jr. (1972). Improvement of the resolution of an instrument by numerical solution of an integral equations. *Journal of Mathematical Analysis and Applications*, **37**, pp. 83-112.

Sideris, M. G. (1984). Computation of gravimetric terrain corrections using fast Fourier transform techniques. UCSE Report #20007, Division of Surveying Engineering, University of Calgary, Calgary, Alberta, Canada.

Sideris, M. G. (1987). Spectral methods for the numerical solution of Molodenskij's problem. UCSE Report #20024, Division of Surveying Engineering, University of Calgary, Calgary, Alberta, Canada.

Sideris, M. G. (1994). Geoid determination by FFT techniques. Lecture Notes for the International School on the Determination and Use of the Geoid, Milan, Italy, October 10-15. International Geoid Service publication

Sjöberg, L. (1975). On the discrete boundary value problem of physical geodesy with harmonic reductions to an internal sphere. The Royal Institute of Technology, Division of Geodesy, Stockholm.

Sjöberg, L. (1979). On the existence of solutions for the method of Bjerhammar in the continuous Case. *Bulletin Géodésique*, **53**, pp. 227-230.

Sjöberg, L. (1984). Least squares modification of Stokes's Veing Meinesz's formulas by accounting for the truncation and potential coefficient errors. *Manuscripta Geodætica*, **9**, pp. 209-229.

Sjöberg, L. (1986). Comparison of some methods of modifying Stokes's formula. *Bollettino Di Geodesia E Scienze Affini*, XLV(**3**), pp. 229-248.

Sjöberg, L. (1991). Refined least squares modification of Stokes's formula. *Manuscripta Geodætica*, **16**, pp. 367-375.

Sjöberg, L. (1998). The exterior Airy/Heiskanen topographic-isostatic gravity potential, anomaly and the effect of analytical continuation in Stokes' formula. *Journal of Geodesy*, **72**, pp. 654-662.

Smeets, I. (1994). An error analysis for the height anomaly determined by combination of mean terrestrial gravity anomalies and a geopotential model. *Bollettino Di Geodesia E Scienze Affini*, **53**, pp. 57-96.

Smithies, F. (1937). The eigenvalues and singular values of integral equations. *Proceedings (London Mathematical Society)*, **43**, pp. 255-279.

Smithies, F. (1965). *Integral Equation*. Cambridge University Press, Cambridge.

Stewart, G. W. (1993). On the early history of the singular value decomposition. *Society for Industrial and Applied Mathematics Review*, **35**, pp. 551-566.

Stokes, G. G. (1849). On the variation of gravity at the surface of the Earth. *Transactions of the Cambridge Philosophical Society*, **VIII**, pp. 672-695.

Strand, O. N. (1974). Theory and methods related to the singular-function expansion and Landweber's iteration for integral equations of the first kind. *SIAM Journal on Numerical Analysis*, **4**, pp. 798-825.

Strand, O. N. and Ed R. Westwater. (1968). The statistical estimation of the numerical solution of a Fredholm integral equation of the first kind. *Journal of the Association for Computing Machinery*, **15**, pp. 100-114.

Strang van Hees, G. L. (1992). Practical formulas for the computation of the orthometric, dynamic and normal heights. *Zeitschrift für Vermessungswesen*, **11**, pp. 727-730.

Sun, W. and P. Vaníček. (1996). On the discrete problem of downward continuation of Helmert's gravity. In: *Techniques for Local Geoid Determination*, eds. I. Tziavos and M. Vermeer. Reports of the Finnish Geodetic Institute, **96:2**, MASALA.

Sun, W. and P. Vaníček. (1998). On some problems of the downward continuation of the $5' \times 5'$ mean Helmert gravity disturbance. *Journal of Geodesy*, **72**, pp. 411-420.

Swick, C. H. (1942). Pendulum gravity measurements and isostatic reductions. U. S. Coast and Geodetic Survey Special Publication 232.

Tapley, B. D., *et al.* (1996). The JGM-3 Geopotential Model. *Journal of Geophysical Research*, **101(B12)**, pp. 28,029-28,049.

Teisseyre, R. (1989). The Earth's gravity field. In: *Gravity and Low-Frequency Geodynamics*, eds. R. Teisseyre, Physics and Evolution of the Earth's Interior, **4**, Elsevier, Amsterdam, Oxford, New York, Toyko.

te Riele, H. J. J. (1985). A program for solving first kind Fredholm integral equations by means of regularization. *Computer Physics Communications*, **36**, pp. 423-432.

Tikhonov, A. H. (1963). Regularization of incorrectly posed problems. *Soviet mathematics - doklady*, **4**, pp. 1624-1627.

Tikhonov, A. H. (1964). Solution of nonlinear integral equations of the first kind. *Soviet mathematics - doklady*, **5**, pp. 835-838.

Tikhonov, A. H. (1965). Nonlinear equations of first kind. *Soviet mathematics - doklady*, **6**, pp. 559-562.

Tikhonov, A. N. and V. H. Arsenin. (1977). *Solutions of Ill-Posed Problems*. Wiley, New York.

Tscherning, C.C. (1976). Covariance Expressions for Second and Lower Order Derivatives of the Anomalous Potential. Rep. **225**, Department of Geodetic Science and Surveying, The Ohio State University, Columbus.

Twomey, S. (1963). On the numerical solution of Fredholm integral equations of the first kind by the inversion of the linear system produced by quadrature. *Journal of the Association for Computing Machinery*, **10**, pp. 97-101.

Vaníček, P., R. O. Castle and E. I. Balazs. (1980). Geodetic levelling and its applications. *Reviews of geophysics and space physics*, **18**, pp. 505-524.

Vaníček, P. and A. Kleusberg. (1987). The Canadian geoid - Stokesian approach. *Manuscripta Geodætica*, **12**, pp. 86-98.

Vaníček, P. and E. J. Krakiwsky. (1986). *Geodesy: the concepts* (2nd edn). North Holland, Amsterdam.

Vaníček, P. and Z. Martinec. (1994). The Stokes-Helmert scheme for the evaluation of a precise geoid. *Manuscripta Geodætica*, **19**, pp. 119-128.

Vaníček, P. and Sjöberg. (1991). Reformation of Stokes's theory for higher than second-degree reference field and a modification of integration kernels. *Geophysical Journal International*, **96**, pp. 6529-6539.

Vaníček, P., and W. E. Featherstone. (1998). Performance of three types of Stokes's kernel in the combined solution for the geoid. *Journal of Geodesy*, **72**, pp. 684-697.

Vaníček, P. Novák and J. Huang. (1997). Atmosphere in Stokes-Helmert's solution of the geodetic boundary-value problem. Contract report for the Geodetic Survey Division, Natural Resources Canada, Ottawa.

Vaníček, J. Huang and P. Novák. (1997). DOWN'97 - Discrete Poisson downward continuation program package for $5' \times 5'$ data. Progress report for the Geodetic Survey Division, Natural Resources Canada, Ottawa.

Vaníček, P., J. Huang, P. Novák, S. Pagiatakis, M. Véronneau, Z. Martinec, W. E. Featherstone. (1999). Determination of the boundary values for the Stokes-Helmert problem. *Journal of Geodesy*, **73**, pp. 180-192.

Vaníček, P. and P. Novák. (1999). Comparison between Planar and Spherical Models of Topography. CGU Annual Meeting in Banff. (Abstract only)

Vaníček, P. and J. Wong. (1999). On the downward continuation of Helmert's gravity anomalies. AGU Annual Meeting in Boston. (Abstract only)

Vaníček, P. and J. Wong. (2000). Error propagations of harmonic downward continuation. In Press.

Varah, J. M. (1973). On the numerical solution of ill-conditioned linear systems with applications to ill-posed problems. *SIAM Journal on Numerical Analysis*, **10**, pp. 257-267.

Vermeer, M. and M. Poutanen. (1996). A modified GRS-80 normal field including permanent tide and atmosphere. Pres. IAG Symposium on Gravity, Geoid and Marine Geodesy (GRAGEOMAR96), Tokyo, Japan, Sep. 28 - Oct 6.

Vogel, C. R. (1986). Optimal choice of a truncation level for the truncated SVD solution of linear first kind integral equations when data are noisy. *SIAM Journal on Numerical Analysis*, **23**, pp. 109-117.

Wahba, G. (1973). Convergence rates of certain approximate solution to Fredholm integral equations of the first kind. *Journal of Approximation Theory*, **7**, pp. 167-185.

Walsh, J. L. (1929). The approximation of the harmonic functions by harmonic polynomials and by harmonic rational functions. *American Mathematical Society*, **35**, pp. 499-544.

Wang, Y. M. (1988). Downward continuation of the free-air gravity anomalies to the ellipsoid using the gradient solution, Poisson's integral and terrain correction-numerical comparison and the computations. Rep. **393**, Department of Geodetic Science and Surveying, The Ohio State University, Columbus.

Wang, Y. M. (1990). The effect of topography of the determination of the geoid using analytical downward continuation. *Bulletin Géodésique*, **64**, pp. 231-246.

Wenzel, G. (1982). Geoid computation by least-squares sepectral combination using integration kernels. Proceedings of the General Meeting of the IAG, Tokyo, PP. 438-453.

Wenzel, G. (1998). Spherical harmonic models. http://www.ife.uni-hannover.de/ wenzel/geopmods.htm

Weyl, H. (1912). Das asymptotische Verteilungsgesetz der Eigenwert linearer partieller Differentialgleichungen (mit einer Anwendung auf der Theorie der Hohlraumstrahlung). *Mathematische Annalen*, **71**, pp. 441-479.

Weyl, H. (1949). Inequalities between the two kinds of eigenvalues of a linear transformation. *Proceedings of the National Academy of Sciences*, **35**, pp. 408-411.

Wichiencharoen, C. (1982). The direct effects on the computation of geoid indulations. Rep. **336**, Department of Geodetic Science and Surveying, The Ohio State University, Columbus.

Wichiencharoen, C. (1984). A comparison of gravimetric geoid undulations computed by the modified Molodensky truncation method and the method and the method of least-squares spectral combination by optimal integration kernel. *Bulletin Géodésique*, **58**, pp. 494-509.

Wing, G. M. (1985). Condition numbers of matrices arising from the numerical solution of linear integral equations of the first kind. *Jounral of Integral Equations (Suppl.)*, **9**, pp. 191-204.

Wing, G. M. (1992). *A Primer on Integral Equations of the First Kind: The Problem of Deconvolution and Unfolding*. SIAM, Philadelphia.

Wong, L. and R. Gore. (1969). Accuracy of geoid heights from modified Stokes kernels. *The Geophysical journal of the Royal Astronomical Society*, **18**(1), pp. 81-91.

Wong, J. and P. Vaníček. (2000). The spectral analysis of the harmonic downward continuation using discrete Picard tecnhique. In Press.

Xu, P. and R. Rummel. (1994). A generalized regularization method with applications in determination of potential fields. *Manuscripta Geodætica*, **20**, pp. 8-20.

Zagrebin, D. W. (1956). *Die theorie des regularisierten geoids*. Veröffentlichungen des Geodätischen Instituts in Postsdam, Nr. 9, Akademie-Verlag, Berlin.

Zakatov, P.S. (1953). *A Course in Higher Geodesy*. Translated from the Russian (1962) by the Israel Program for Scientific Translations, Jerusalem, for Office of Technical Services, Department of Commerce, Washington, DC.

Appendix

Appendix A

Eigenvalue System

The goal of the Appendix A is to summarize two eigenvalue systems, Eigenvalue Exanpasion (EVE) and Quasi-Eigenvalue Decomposition (QEVD), and their general properties.

A.1   Eigenvalue Expansion (EVE)

In this part we shall focus on the following expression:

$$T(\Omega) = \int_{\Omega'} K(r, \psi, R) T(\Omega') d\Omega',$$

instead of Eq. (1.1.7), and the integral operator $\mathcal{K}$ is defind by:

$$\mathcal{K}T(\Omega) = \int_{\Omega'} K(r, \psi, R) T(\Omega') d\Omega', \tag{A.1.1}$$

in a $\mathcal{L}^2$-space setting. Define the inner product:

$$(T_1, T_2) = \int_{\Omega} T_1(\Omega) T_2(\Omega) d\Omega.$$

The adjont operator $\mathcal{K}^*$ is easily found to be:

$$\mathcal{K}T(\Omega') = \int_{\Omega'} K(r, \psi, R) T(\Omega') d\Omega'. \tag{A.1.2}$$

A Possion kernel K is a square integrable function if its norm exists and has an EVE which is a mean convergent expansion in the form:

$$K(r, \psi, R) = \sum_{j=2}^{\infty} \left(\frac{R}{r}\right)^{j+1} \sum_{m=-j}^{j} Y_{jm}(\Omega) Y_{jm}^{*}(\Omega') \qquad (A.1.3)$$

in which is a sequence of spherical harmonic functions $Y_{jm}(\Omega), Y_{jm}(\Omega')$, called eigenfunctions, and radial attenuation factors $(R/r)^{j+1}$, called eigenvalues, satisfying:

1.

$$\int_{\Omega} Y_{j_1 m_1}^{*}(\Omega) Y_{j_2 m_2}(\Omega) d\Omega = \delta_{j_1 j_2} \delta_{m_1 m_2} = \begin{cases} 1 & \text{if } j_1 = j_2 \text{ and } m_1 = m_2, \\ 0 & \text{if } j_1 \neq j_2 \text{ and } m_1 \neq m_2. \end{cases} \qquad (A.1.4)$$

2.

$$\int_{\Omega'} Y_{j_1 m_1}^{*}(\Omega') Y_{j_2 m_2}(\Omega') d\Omega' = \delta_{j_1 j_2} \delta_{m_1 m_2} = \begin{cases} 1 & \text{if } j_1 = j_2 \text{ and } m_1 = m_2, \\ 0 & \text{if } j_1 \neq j_2 \text{ and } m_1 \neq m_2. \end{cases}$$

$$(A.1.5)$$

3. The non-increasing order of the eigenvalues is:

$$\underbrace{\left(\frac{R}{r}\right)}_{\text{Large}} \geq \left(\frac{R}{r}\right)^{2} \geq \cdots \geq \left(\frac{R}{r}\right)^{j} \geq \left(\frac{R}{r}\right)^{j+1} \geq \underbrace{\cdots}_{\text{Smaller and Smaller}} \qquad (A.1.6)$$

4.

$$\mathcal{K} Y_{jm}(\Omega') = \left(\frac{R}{r}\right)^{j+1} Y_{jm}(\Omega), \qquad (A.1.7)$$

Or

$$\frac{1}{4\pi} \int_{\Omega'} K(r, \psi, R) Y_{jm}(\Omega') d\Omega' = \left(\frac{R}{r}\right)^{j+1} Y_{jm}(\Omega). \qquad (A.1.8)$$

5.

$$\mathcal{K}^* Y_{jm}(\Omega) = \left(\frac{R}{r}\right)^{j+1} Y_{jm}(\Omega'), \qquad (A.1.9)$$

Or

$$\frac{1}{4\pi} \int_\Omega K^*(r, \psi, R) Y_{jm}(\Omega) d\Omega = \left(\frac{R}{r}\right)^{j+1} Y_{jm}(\Omega'). \qquad (A.1.10)$$

The product of $\mathcal{K}$ and $\mathcal{K}^*$, say $\mathcal{K}\mathcal{K}^* \equiv \mathcal{K}^*\mathcal{K}$ can be converted into:

$$
\begin{aligned}
\| K \|^2 &= \left(\frac{1}{4\pi}\right)^2 \int_\Omega \int_{\Omega'} K(r, \psi, R) K^*(r, \psi, R) d\Omega' d\Omega \\
&= \left(\frac{1}{4\pi}\right)^2 \int_\Omega \int_{\Omega'} 4\pi \sum_{j_1=2}^{\infty} \left(\frac{R}{r}\right)^{j_1+1} \sum_{m_1=-j_1}^{j_1} Y_{j_1 m_1}(\Omega) Y_{j_1 m_1}^*(\Omega') \\
&\quad \times 4\pi \sum_{j_2=2}^{\infty} \left(\frac{R}{r}\right)^{j_2+1} \sum_{m_2=-j_2}^{j_2} Y_{j_2 m_2}^*(\Omega) Y_{j_2 m_2}(\Omega') d\Omega' d\Omega \\
&= \sum_{j=2}^{\infty} \left(\frac{R}{r}\right)^{2j+2} \qquad (A.1.11)
\end{aligned}
$$

which is nothing else than the $\mathcal{L}^2$-norm $\| K \|^2$ in term of the square eigenvalues $\left(\frac{R}{r}\right)^{2j+2}$.

A.2   Quasi-Eigenvalue Decomposition (QEVD)

The QEVD of a real $n \times n$ matrix $\mathbf{B}$ is the factorization as a product of three matrices:

$$\mathbf{B} = \mathbf{U}\Lambda\mathbf{V}^{\mathbf{T}} \qquad (A.2.12)$$

$$
= \begin{bmatrix} \mathbf{u}_1 & \mathbf{u}_2 & \cdots & \mathbf{u}_n \end{bmatrix}_{n \times n}
\begin{bmatrix}
\lambda_1 & 0 & & \cdots & 0 \\
0 & \lambda_2 & \ddots & & \vdots \\
& & \ddots & \ddots & \ddots \\
\vdots & & \ddots & \ddots & 0 \\
0 & \cdots & & 0 & \lambda_n
\end{bmatrix}_{n \times n}
\begin{bmatrix}
\mathbf{v}_1 \\
\mathbf{v}_2 \\
\vdots \\
\mathbf{v}_n
\end{bmatrix}_{n \times n}
\qquad (A.2.13)
$$

The matrices in this factorization have the following properties:

1. $\mathbf{U}$ and $\mathbf{V}$ are orthogonal matrices. The columns $\mathbf{u}_i$ of $\mathbf{U} = [\mathbf{u}_1 \ \mathbf{u}_2 \ \cdots \ \mathbf{u}_n]$ are the left-eigenvectors, and the columns $\mathbf{v}_i$ of $\mathbf{V} = [\mathbf{v}_1 \ \mathbf{v}_2 \ \cdots \ \mathbf{v}_n]$ are the right-eigenvectors. (i.e., $\mathbf{U}\mathbf{U}^\mathbf{T} = \mathbf{I}$, $\mathbf{V}^\mathbf{T}\mathbf{V} = \mathbf{I}$, but $\mathbf{U}\mathbf{V}^\mathbf{T} \neq \mathbf{I}$)

2. Λ is an $n \times n$ diagonal matrix containing the eigenvalues of $\mathbf{B}$, which are defined as the real and non-negative scalars of the eigenvalues of $\mathbf{B}$, where

$$\underbrace{\lambda_1}_{\text{Large}} \geq \lambda_2 \geq \cdots \geq \lambda_i \geq \lambda_{i+1} \geq \underbrace{\cdots}_{\text{Smaller and Smaller}} \geq \lambda_n \qquad (A.2.14)$$

3.

$$\mathbf{u}_i^T \mathbf{u}_j = \delta_{ij} = \begin{cases} \mathbf{1} & \text{if } i = j, \\ 0 & \text{if } i \neq j. \end{cases} \qquad (A.2.15)$$

4.

$$\mathbf{v}_i^T \mathbf{v}_j = \delta_{ij} = \begin{cases} \mathbf{1} & \text{if } i = j, \\ 0 & \text{if } i \neq j. \end{cases} \qquad (A.2.16)$$

5.

$$\mathbf{B}\mathbf{v}_i = \lambda_i \mathbf{u}_i \qquad (A.2.17)$$

$$\mathbf{B}^\mathbf{T}\mathbf{u}_i = \lambda_i \mathbf{v}_i. \qquad (A.2.18)$$

The matrix norm that corresponds to the norm $\| \mathbf{B} \|$ is the Frobenius norm (or largest absolute value) $\| \mathbf{B} \|_F$ defined by:

$$\| \mathbf{B} \|_F = \left(\sum_{i=1}^{n} \lambda_i \right)^{\frac{1}{2}} \qquad (A.2.19)$$

which is equal to the square root of the sum of eigenvalues.

Appendix B

Helmert Gravity Anomaly

B.1 Introduction

In the following a list of important conclusions is based on the latest work of Vaníček *et al.* (1999). Including, some original conceptions and formulæ are slightly modified by the author. The reader should consult the original copy and references therein.

B.1.1 The Helmertization Scheme

The first result in which we use this thesis concerns the masses located outside the geoid, as described by the actual (or real) space. Transformed the "actual space" into the "Helmert space" through one of the existing mass reduction techniques, this procedure can be done by the Helmert 2nd condensation scheme. The masses between two bounded regions are removed and then formed *infinite* numbers of thin condensed layers which are directly proportional to *infinite* numbers of orthometric heights projecting onto the surface of the geoid, as described by the Newton gravitational surface potential V^c. In order to bring a clear picture of the gravitational effect of the topographical masses located between the Earth's topography and the geoid and of the

gravitational effect of the atmospherical masses between a bounding sphere and the geoid, there are two similar approaches to construct the so-called residual potential, *topographical* and *atmospherical*.

- The residual topographical potential δV^t is defined by the Newton gravitational potential V^t caused by the topographical masses subtracting the Newton gravitation surface potential V^c. For more in-depth information on topographical effect, see Wichiencharoen (1982), Kleusberg and Vaníček (1991), Heck (1991a), Martinec *et al.* (1993), Martinec and Vaníček (1994a, 1994b), Vaníček and Martinec (1994), Novák (1999).

- The residual atmospherical potential δV^a is defined by the Newton gravitational potential V^a caused by the atmospherical masses subtracting the Newton gravitation (surface) potential V^{ac} caused by the surface density. For more detailed information on atmospherical effect, see Ecker (1968), Ecker and Mittermayer (1969), Madden (1972), Moritz (1974), Anderson *et al.* (1975), Rummel and Rapp (1976), Diviš *et al.* (1981), Balmino (1983), Vaníček *et al.* (1997), Sjöberg, (1998), Novák (1999).

Adding the gradients of these residual potentials to the magnitude of a Helmert gravity vector, $g^h(r_t, \Omega) = |\text{grad } W^h|_{(r_t,\Omega)} = |\text{grad}(W + \delta V^t + \delta V^a)|_{(r_t,\Omega)} \in \Gamma_t$ is fulfilled the physical counterpart of harmonicity (Vaníček *et al.*, 1999). Then, taking the difference between the magnitudes of $g^h(r_t, \Omega)$ and normal gravity vector $\gamma([r_t - Z^h(r_t, \Omega)], \Omega) = |\text{grad } U|_{[r_t - Z^h(r_t,\Omega)]} \in \Gamma_e$, where Γ_e denotes a bounded domain of reference ellipsoid of revolution, is defined by a Helmert gravity anomaly $\Delta g^h(r_t, \Omega)$ (ibid.).

B.1.2   The Linearization Procedure

The second finding concerns the GBVP, referred to as a non-linear free tpye.

1. GBVP is a non-linear physical phenomenon which aries from the non-linearization procedure of $g^h(r_t, \Omega)$ and $\gamma([r_t - Z^h(r_t, \Omega)], \Omega)$.

Helmert Gravity In the first place, the Helmert gravity belongs to a non-linearly annular region between on the Earth's topography as well as the geoid. When expressing $g^h(r_t, \Omega)$, or the gradient of a *combinational potential*, which consists of a gravity potential W, the residual topographical potential δV^t and the residual atmospherical potential δV^a in a Maclaurin series expansion:

$$
\begin{aligned}
g^h(r_t, \Omega) &= |\mathrm{grad}(W + \delta V^t + \delta V^a)| \\
&= |\mathrm{grad}W| \left[1 + 2\frac{\mathrm{grad}W \cdot \mathrm{grad}(\delta V^t + \delta V^a)}{|\mathrm{grad}W|^2} + \frac{|\mathrm{grad}(\delta V^t + \delta V^a)|^2}{|\mathrm{grad}W|^2}\right]^{1/2} \\
&= |\mathrm{grad}W| \left[1 + \frac{\mathrm{grad}W \cdot \mathrm{grad}(\delta V^t + \delta V^a)}{|\mathrm{grad}W|^2} + \mathcal{O}\left(\frac{|\mathrm{grad}(\delta V^t + \delta V^a)|}{|\mathrm{grad}W|}\right)^2\right],
\end{aligned}
$$

with respect to the geocentric radius, omitting second and higher order derivatives of $|\mathrm{grad}(W + \delta V^t + \delta V^a)|$ reading that the term:

$$
\left|\frac{\mathrm{grad}(\delta V^t + \delta V^a)}{\mathrm{grad}W}\right|
$$

is sufficiently smaller than 1. And taking a chosen point on the Earth's topography as follows:

$$
g^h(r_t, \Omega) \doteq g(r_t, \Omega) + \left.\frac{\vec{g} \cdot \mathrm{grad}(\delta V^t + \delta V^a)}{g}\right|_{(r_t, \Omega)}. \tag{B.1.1}
$$

Finally, the Helmert gravity is defined by:

$$
g^h(r_t, \Omega) \doteq g(r_t, \Omega) + \left.\frac{\partial \delta V^t}{\partial r}\right|_{(r_t, \Omega)} + \left.\frac{\partial \delta V^a}{\partial r}\right|_{(r_t, \Omega)},
$$

or shortly

$$
\doteq g(r_t, \Omega) + \delta \mathcal{A}^t(r_t, \Omega) + \delta \mathcal{A}^a(r_t, \Omega), \tag{B.1.2}
$$

where the two linearized terms are called the *direct topographical effect* and the *direct atmospherical effect*.

78

Normal Gravity The marriage between the Molodenskij-Hirvonen theory of the normal height H^N in connection with the quasi-geoid (Molodenskij *et al.*, 1960) and telluroid (Hirvonen, 1960), and the Stokes theory of the orthometric height H^O with reference to the geoid in an actual space seemed to be forgotten for a while in a geodetic literature. It was Vaníček *et al.* in 1999 who used them as a vechicle for introducing the *correction for the orthometric height* under a spherical approximation, and defined a so-called Helmert normal height $(H^N)^h(\Omega)$ in concert with a Helmert telluroid in the Helmert space setting because (1) such a so-called simple Bouguer anomaly $\Delta g^{SB}(\Omega)$ is to be employed, (2) the trade-off between H^N and H^O is linked into two *indirect*[1] residual potential corrections.

In what follows, the normal gravity locates at a non-linearly annular region between on the Helmert telluroid at the Helmert normal height $(H^N)^h(\Omega)$ as well as on the equipotential surface at the orthometric height $H^O(\Omega)$, above the reference ellipsoid, respectively. When expanding $\gamma([r_t - Z^h(r_t, \Omega)], \Omega)$, which is equivalent to $\gamma([r_E + (H^N)^h(\Omega)], \Omega)$ (Vaníček *et al.*, Eq. (29), 1999), $r_t(\Omega) = R + H^O(\Omega)$, r_E is a radius of ellipsoid, in a Taylor series expansion with regard to a position of $([r_E + H^O(\Omega)], \Omega)$ such that

$$
\gamma([r_t - Z^h(r_t, \Omega)], \Omega)
$$
$$
= \gamma([r_E + (H^N)^h(\Omega)], \Omega)
$$
$$
= \gamma([r_E + H^O(\Omega)], \Omega) + \left. \frac{\partial \gamma}{\partial n} \right|_{([r_E + H^O(\Omega)], \Omega)} [r_E + (H^N)^h(\Omega) - r_E - H^O(\Omega)]
$$
$$
+ \frac{1}{2!} \left. \frac{\partial^2 \gamma}{\partial n^2} \right|_{([r_E + H^O(\Omega)], \Omega)} [r_E + (H^N)^h(\Omega) - r_E - H^O(\Omega)]^2 + \cdots .
$$

A linear model but a weak linearity comes into play when terms of second and high order may be no longer taken into consideration but rather

---

[1] In geodetic literature, the terminology of the direct and indirect effects in the actual space seems to be confused its content to the reader from time to time. According to Pick, Pícha and Vyskočil's definition (1973), the former refers to the topographical corrections the layer bewteen the Earth's topography and the geoid, while the latter the layer between the the quasi-geoid and the geoid.

the first term are still remained in the series:

$$\gamma([r_t - Z^h(r_t, \Omega)], \Omega)$$

$$\doteq \gamma([r_E + H^O(\Omega)], \Omega) + \left.\frac{\partial \gamma}{\partial n}\right|_0 [(H^N)^h(\Omega) - H^O(\Omega)],$$

where the subscript 0 denotes that the vertical gradient of normal gravity is approximately evaluated on the reference ellipsoid, under a spherical approximation and using (ibid., Eq. (36)):

$$\doteq \gamma([r_E + H^O(\Omega)], \Omega) - \frac{2}{R}H^O(\Omega)\Delta g^{SB}(\Omega) - \frac{2}{R}\delta V^t(r_t, \Omega) - \frac{2}{R}\delta V^a(r_t, \Omega)$$

$$= \gamma([r_E + H^O(\Omega)], \Omega) - \frac{2}{R}H^O(\Omega)\Delta g^{SB}(\Omega) - \delta\mathcal{I}^t(r_t, \Omega) - \delta\mathcal{I}^a(r_t, \Omega).$$

$$(B.1.3)$$

After a proper linearization has taken place, perturbation theory can be applied to evaluate different sources of corrections up to certain level of reasonable accuracy in a view of 1 cm starting from first-order term estimations in the original expansion. In an ascending order from the last expression, there are called the correction for the *difference between the quasi-geoid and the geoid in an actual space* plus the correction for the *second indirect topographical* (and *atmospherical*) *effects* on gravity at the Earth's topography. Physically speaking, the two indirect effects on gravity indicate that the curvature of equipotential surface $2/R$ is directly proportional to the boundary displacement of two residual potential values.

2. GBVP is a free boundary value problem since the unknown surface of the Helmert gravity anomalies located on the Helmert co-geoid to be determined bases on the distribution of the *discrete* observed gravity values on the Earth's topography in the sense of Bjerhammer (1976).

The non-linear free boundary value problem is boiled down to the linear free boundary value problem. Of particular interest is the non-stability of the linear free

boundary value problem by asking the question of whether or not the convergence of the unknown physical surfaces, as described by the approximants by expressing the linearization aftermath and then taking higher and higher order derivatives of $g^h(r_t, \Omega)$ and $\gamma([r_t - Z^h(r_t, \Omega)], \Omega)$ at a chosen point (r_t, Ω) and $([r_E + H^O(\Omega)], \Omega)$, but still remains to be examined in term of analytical continuation (Heck, 1991b; Martinec, 1998).

B.1.3   The Usage of Complete Bouguer Anomaly

The partnership on the use of *complete Bouguer anomaly* $\Delta g^{CB}(\Omega)$ between the geophysical and geodetic literatures (Hipkin, 1988) brings us astray by the misconception of mass reduction procedure to provide other puzzling question. As illustrated by LeFehr (1991a, 1991b) and (ibid.), the values $\Delta g^{CB}(\Omega)$ are *station anomalies*, which do not have as a purpose the mass reduction of the data to the Helmert co-geoid. The complete Bouguer anomaly is defined as:

$$\Delta g^{CB}(\Omega) = \Delta g^{SB}(\Omega) + \delta g^{tc}(r_t, \Omega),$$

where $\delta g^{tc}(r_t, \Omega)$ is the gravimetric *terrain correction* for departures of the Earth's topography from a corresponding spherical approximation surface, and $\Delta g^{SB}(\Omega)$ is consisted of four components (Swick, 1942):

1. The observed gravity $g(r_t, \Omega)$,

2. The normal gravity $\gamma([r_E + H^O(\Omega)], \Omega)$. Using the Taylor series expansion of $\gamma([r_E + H^O(\Omega)], \Omega)$ with regard to a position of $\gamma(r_E, \Omega)$, the linearized term becomes:

$$\gamma([r_E + H^O(\Omega)], \Omega) \doteq \gamma(r_E, \Omega) + \left.\frac{\partial \gamma}{\partial n}\right|_{(r_E, \Omega)} H^O(\Omega),$$

   where $\left.\frac{\partial \gamma}{\partial n}\right|_{(r_E, \Omega)} H^O(\Omega) = -0.3086 H^O(\Omega)$ mGal is the Free-air reduction. The dilemma between the Free-air reduction and two direct topographical/amtospherical

effects on gravity is a significantly physical difference. The former does not shave off all mass down to the geoid, but rather interprets in light of gravity variation with altitude (LaFehr *et al.*, 1986); the latter, however, does play a key-rôle of gravity correction under the influence of these topographical/amtospherical masses above the geoid,

3. The simple Bouguer slab (plate) formula $2\pi\varrho_0 G H^O(\Omega)$, where ϱ_0 is a rock density of 2.68 g/cm^3 above the geoid. Does the simple Bouguer correction is given by an infinite slab formula or a spherical form? This question was answered in 1971 by Karl, and is recently given further thought in 1999 by Vaníček *et al.*. However, it is still an open question under consideration to be solved,

4. A curvature effect $8\pi\varrho_0 G[H^O(\Omega)]^2/R$, but not considered in practice because of having a small effect (Bullard, 1936; Vaníček and Krakiwsky, 1986).

To sum up, we have:

$$\Delta g^{CB}(\Omega) = g(r_t, \Omega) - \gamma([r_E + H^O(\Omega)], \Omega) - 2\pi\varrho_0 G H^O(\Omega) + \delta g^{tc}(r_t, \Omega). \quad \text{(B.1.4)}$$

Making the difference between Eqs. (B.1.2) and (B.1.3) and applying Eq. (B.1.4), the *pre*-Helmert gravity anomaly is given as:

$$\begin{aligned}
\Delta g^h(r_t, \Omega) = {} & \Delta g^{CB}(\Omega) + 2\pi\varrho_0 G H^O(\Omega) - \delta g^{tc}(r_t, \Omega) \\
& + \frac{2}{R} H^O(\Omega) \Delta g^{SB}(\Omega) + \delta\mathcal{I}^t(r_t, \Omega) + \delta\mathcal{I}^a(r_t, \Omega) \\
& + \delta\mathcal{A}^t(r_t, \Omega) + \delta\mathcal{A}^a(r_t, \Omega).
\end{aligned}$$

Grouping the difference between the direct topographical effect and the gravimetric terrain correction, known as the *condensed terrain effect* $\delta\mathcal{A}^{cr}(r_t, \Omega)$:

$$\delta\mathcal{A}^t(r_t, \Omega) - \delta g^{tc}(r_t, \Omega) = \delta\mathcal{A}^{cr}(r_t, \Omega), \quad \text{(B.1.5)}$$

is defined by (Vaníček *et al.*, 1999). Finally, the Helmert gravity anomaly on the Earth's topography is given as :

$$\Delta g^h(r_t, \Omega) := \Delta g^{CB}(\Omega) + 2\pi \varrho_0 G H^O(\Omega) + \frac{2}{R} H^O(\Omega) \Delta g^{SB}(\Omega)$$
$$+ \delta \mathcal{I}^t(r_t, \Omega) + \delta \mathcal{I}^a(r_t, \Omega) + \delta \mathcal{A}^a(r_t, \Omega) + \delta \mathcal{A}^{cr}(r_t, \Omega). \qquad \text{(B.1.6)}$$

Appendix C

$\mathcal{L}^2$-Norm

It has been known for some time that in 3-D harmonic upward and downward continuation a linear Fredholm integral equation of the first kind is employed (Wing, 1992; Bitsadze, 1995). The prototypic form of its mathematical expression is:

$$\text{Physical Output}\big|_{\overset{\top}{\oplus}} := \frac{1}{4\pi} \int_{\Omega} \text{Physical Input}\big|_{\overset{\perp}{\oplus}} \times \text{ Geometical Configuration } d\Omega$$

(C.0.1)

where Ω is a closed/perodic interval on the surface of the sphere, $\overset{\top}{\oplus}$ and $\overset{\perp}{\oplus}$ represent the external and internal geometry, respectively. The product of Physical Input and Geometical Configuration with the normalization factor $1/4\pi$ integrating over the the bounding sphere with respect to the origin is equal to the mean area on the skin of the sphere in a global sense.

Beginning with a rudimentary assumption, it is important to choose appropriate function spaces for given functions and functions to be determined according to a given kernel (namely a geometrical configuration function) as well as to introduce an appropriate norm for measuring the continuous dependence. Throughout the thesis, let us assume that the spaces $\mathcal{L}^2(\mathcal{W}, \mathbb{R}^3)$, $\mathcal{L}^2(\mathcal{Q}, \mathbb{S}^2)$ consist of all functions {Physical Output} $\in \mathcal{W}$, and {Physical Input} $\in \mathcal{Q}$ whose $\mathcal{L}^2$-norm $\| \cdot \|_{\mathcal{L}^2(\cdot,\cdot)}$ (2-nd power, or energy norm) is *square integrable* (s.i.) (or square root of sum of squares)

in the domain $\mathcal{W}$, and on the surface $\mathcal{Q}$ defined in $\mathbb{R}^3$, and on $\mathbb{S}^2$, respectively if the corresponding norms

$$\| \text{ Physical Input } \|_{\mathcal{L}^2(\mathcal{Q},\mathbb{S}^2)} \equiv \left(\int_\Omega |\text{Physical Input}|^2 \, d\Omega \right)^{1/2} < +\infty,$$

and

$$\| \text{ Physical Output } \|_{\mathcal{L}^2(\mathcal{W},\mathbf{R}^3)} \equiv \left(\int_{\Omega'} |\text{Physical Output}|^2 \, d\Omega' \right)^{1/2} < +\infty$$

are finite and exist, where Physical Input and Physical Output are functions of positions, (r, Ω) and (R, Ω'), respectively such that

$$(r, \Omega) := \{ r \in [R, R + H^O(\Omega)) \text{ and } \Omega = (\varphi, \lambda) |\ 0 \le \varphi \le 2\pi, 0 \le \lambda \le \pi \} \subset \mathbb{R}^3,$$

and

$$(R, \Omega') := \{ R \text{ is fixed and } \Omega' = (\varphi', \lambda') |\ 0 \le \varphi' \le 2\pi, 0 \le \lambda' \le \pi \} \subset \mathbb{S}^2.$$

Similarity, a Geometical Configuration function $\in \mathcal{L}^2(\mathcal{W}, \mathbb{R}^3) \times \mathcal{L}^2(\partial\mathcal{Q}, \mathbb{S}^2)$ is s.i. if its norm exists, i.e.:

$$\| \text{ Geometical Configuration } \|_{\mathcal{L}^2(\mathcal{W},\mathbf{R}^3) \times \mathcal{L}^2(\mathcal{Q},\mathbb{S}^2)}$$
$$\equiv \int_\Omega \int_{\Omega'} |\text{ Geometrical Configuration}|^2 \, d\Omega' d\Omega < +\infty$$

This $\mathcal{L}^2$ setting for the HDC is associated closely with the context in which linear Fredholm integral equations of the first kind are not only often closely related to the definition of Picard criterion for analyzing the existence of a solution of the right-hand side of Eq. (C.0.1) but is also much closer to the reality of the measured size of the physical quantities. Without any mathematical trickery the behaviour of physical disturbance for the input and output is as close as possible together.

Full Name: Jeff Chak Fu Wong

Place and Date of Birth: Hong Kong, April 8, 1970.

Permanent Address:

No. 43, 2$^{\text{nd}}$ Floor

Chung Mei Village, Tsing Yi Island

Hong Kong, China

College and Universities Attended:

Red Deer College

Red Deer, Alberta

1992-1994, First and Second Years in Engineering Program

University of Calgary

Calgary, Alberta

1994, Spring and Summer Studies in Engineering Program

Department of Mathematics

University of New Brunswick

Fredericton, New Brunswick

1994-1996, B.Sc. in Mathematics

Department of Mathematical Sciences

University of Alberta

Edmonton, Alberta

1997, Visiting Student in Mathematics

Publications:

Vaníček, P. and J. Wong. (1999). On the downward continuation of Helmert's gravity anomalies. AGU Annual Meeting in Boston. (Abstract only)